Fatigue life prediction methodology for L-flange connection under different preload levels based on crack growth analysis

Iman Shakeri, Hagar El Bamby, Trayana Tankova, Milan Veljkovic : Delft University of Technology
Rajab Said, Chris Timbrell : Zentech International Limited

NAFEMS UK Conference 18-19 May 2026

Contents

NAFEMS

45 Years Supporting a Safer, Greener & More Innovative Future

Supporting Established & Emerging Industries Worldwide

Academia

Aerospace

Biomedical Engineering

Defence

Energy & Infrastructure

Ground Transportation

Material & Manufacturing

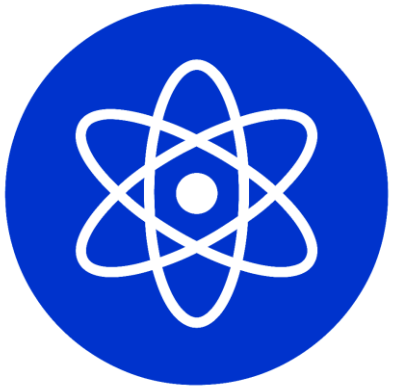

Nuclear

Oil & Gas

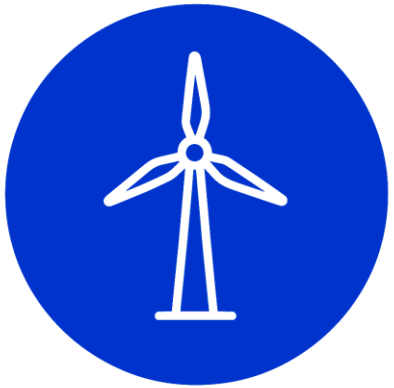

Renewable Energy

From Manufacturing Defects to Structural Performance

Hartman- Schijve Model

Additive Mfg

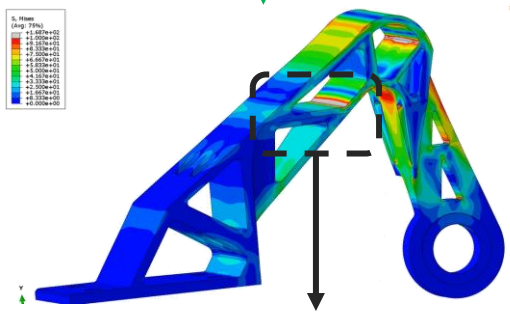

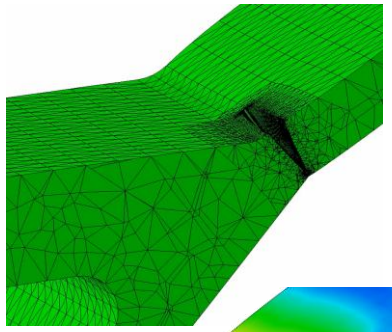

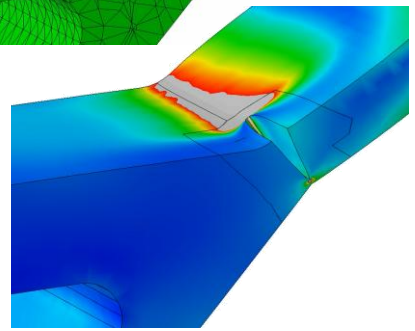

Composites

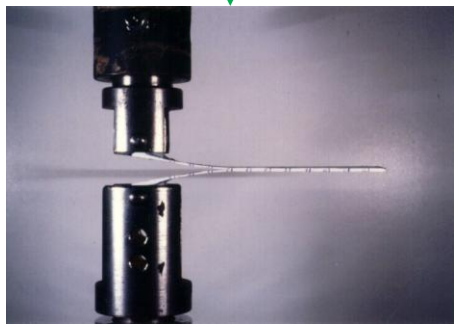

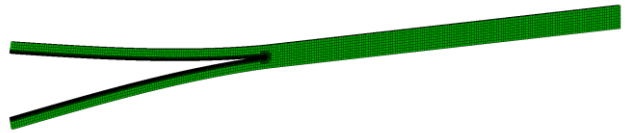

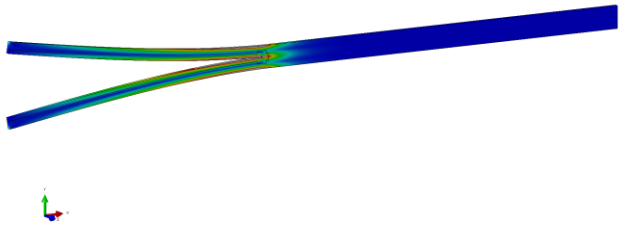

Rhys Jones et al:
https://doi.org/10.3390/ma19020372

Ramesh Chandwani et al:
0.1016/j.tafmec.2026.105487

Process → Microstructure → Performance

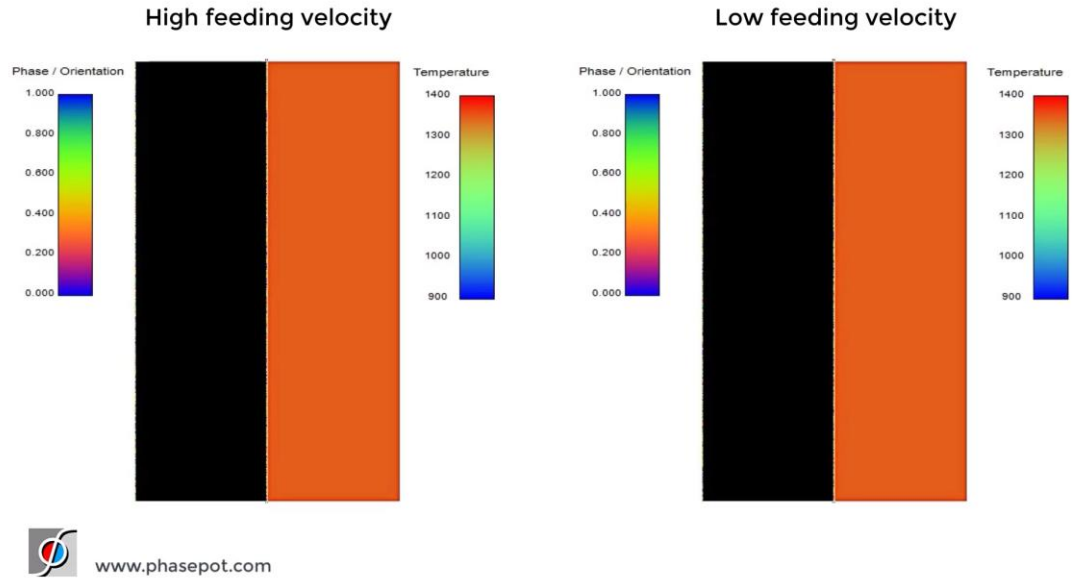

www.phasepot.com

Rautomead: Vertically Upward Continuous Cast – control process speed

PhasePot

Strategic partnership:
See our join project (IDEGAIT) at Session **3A**

Wind turbine vs durability and reliability

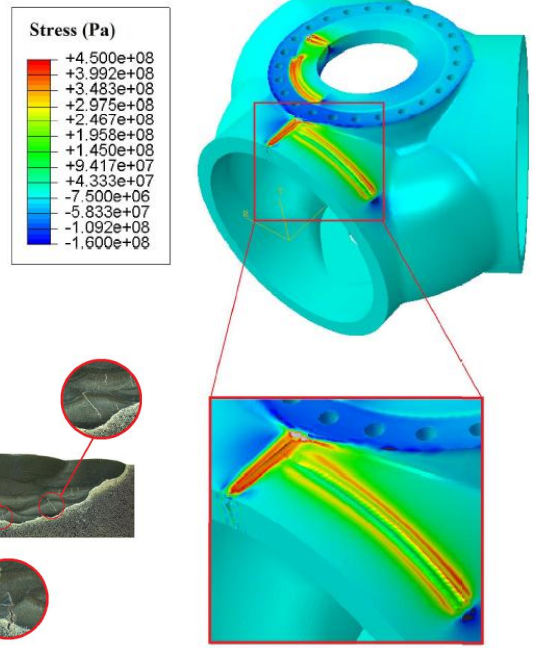

Weld repair vs microcracks..!

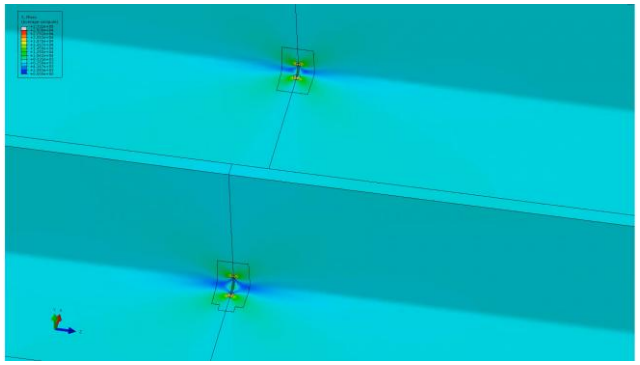

Composites – Blade stiffeners

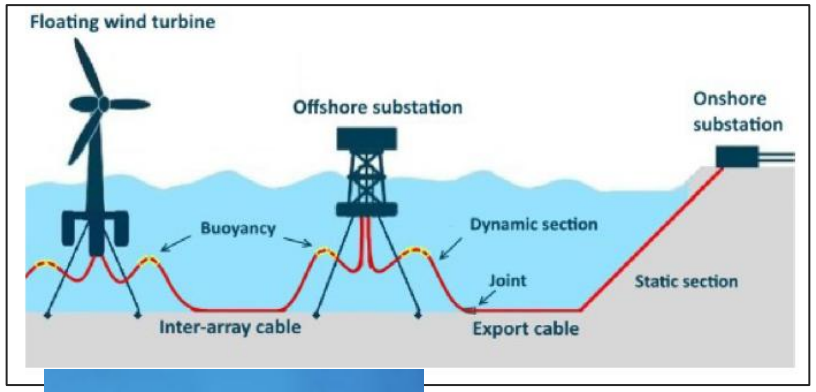

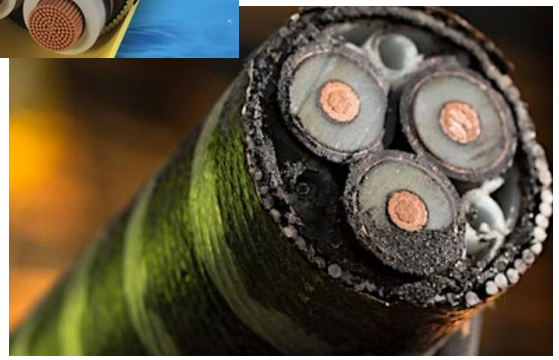

Offshore - Harsh(er) environment with subsea and floating structures

Tower-joint failure..?!!

Introduction

- Offshore wind turbines are increasingly required to operate beyond their original design life, placing renewed emphasis on structural integrity and fatigue performance
- Bolted L-flange connections used to assemble tower sections are a key structural detail
  - complex combinations of axial and bending load induced by wind, wave action and rotor dynamics
  - bolt preload helps mitigate against fatigue damage but actual preload often deviates from the design value due to uncertainties in the tightening process and geometric imperfections

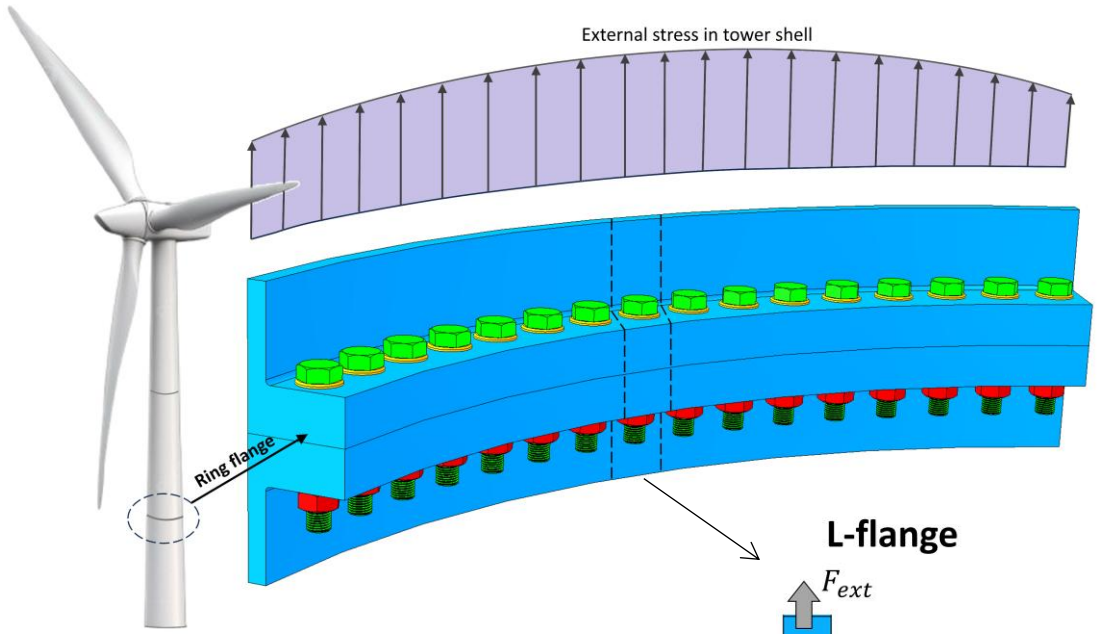

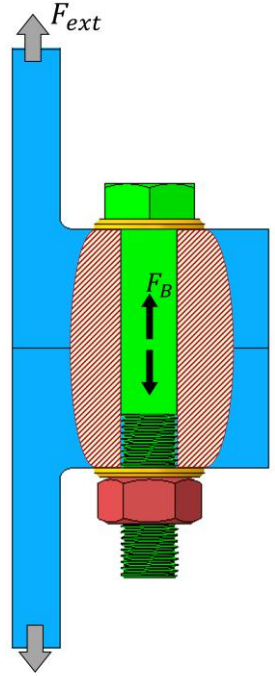

Current design standards provide conservative fatigue guidance, but they remain largely empirical and do not explicitly account for preload variability, preload loss, or crack-growth behaviour at the thread root

Introduction

- The work summarized in this presentation is recent research carried out at Delft University of Technology, adopting a fracture-mechanics framework
  - Realistic bolt and thread geometries are explicitly represented, enabling accurate evaluation of load transfer function (LTF), crack evolution and stress intensity factor (SIF)
  - The methodology combines 3D FE modelling in Abaqus with automated fracture-mechanics analysis using Zencrack
  - Parameterisation of key FEA results allows creation of synthetic S-N curves accounting for effect of preload loss and crack development
- Full details are published in:
  - Thin-Walled Structures, Volume 217, Part B, December 2025, 113893
  - For equations whose details are beyond the scope of these slides
    - The published paper provides the full background to all terms and equations
    - Equation numbers in these slides are retained as per the published paper

L-flange connection

- Preload is the initial tensile load in the bolt after tightening
  - Induces clamping force between components
  - Allows external load to be primarily transferred through friction at the interface rather than through the bolt – thus reducing stress fluctuations in the bolt under cyclic loading
- The load transfer function (LTF) describes the relationship between the external force on the tower shell, F_{ext}, and the force experienced by the bolt, F_B
- Deviations in preload can lead to accelerated fatigue damage

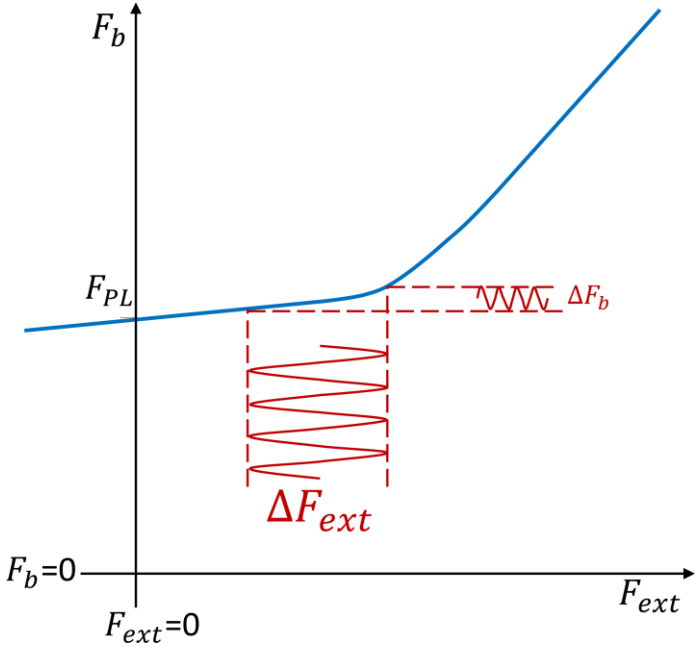

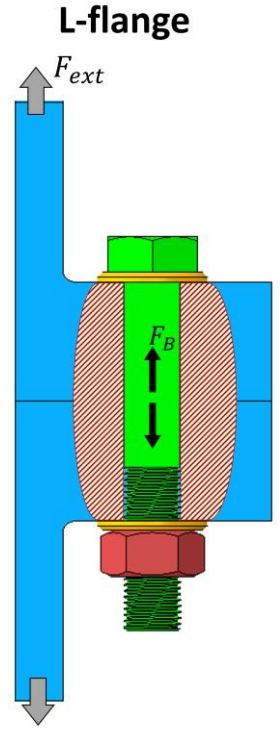

L-flange connection

- Existing fatigue standards such as Eurocode 3 and DNV-RP-203 do not cater for loss of preload or the explicit influence of bending interactions in L-flange connections
- Gaps in understanding:
  - The lack of stress intensity factor solutions for an equivalent 3D semi-elliptic crack subject to axial and bending load in bolted connections with realistic thread geometry
  - Effect of bending caused by load eccentricity on fatigue behaviour and crack propagation
  - The influence of preload loss on fatigue life
- Work aims to predict the stress intensity factors (SIF) and load transfer function (LTF) to enable prediction of fatigue life

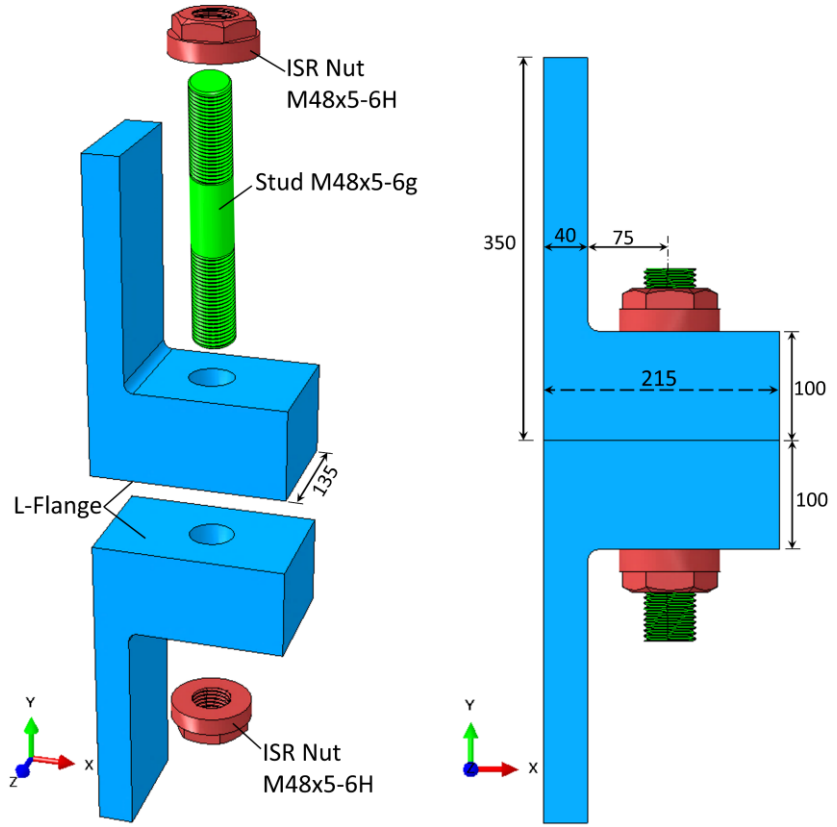

M48 partially threaded stud and ISR nut:

5mm pitch
Stud major and minor diameters: 47.7mm and 41.9mm
Nut major and minor diameters: 48.5 and 42.9mm
Stud unthreaded section: 112mm with diameter 45mm
Nut outer diameter: 92mm

Material:

E 210GPa, ν 0.3
Elastic-plastic with isotropic hardening (preload simulations)

L-flange connection

1. **Stress intensity factor calculation**
   Axisymmetric and helical thread FEA
2. **Stress intensity factor parameterisation**
   Parameterisation of FEA results
3. **Preload assessment**
   Global model and submodel FEA
4. **Preload effect on load transfer function**
   Parameterisation of preload results
5. **Preload effect on fatigue life**
   Calculation of fatigue life

NAFEMS

Summary of Zencrack workflow

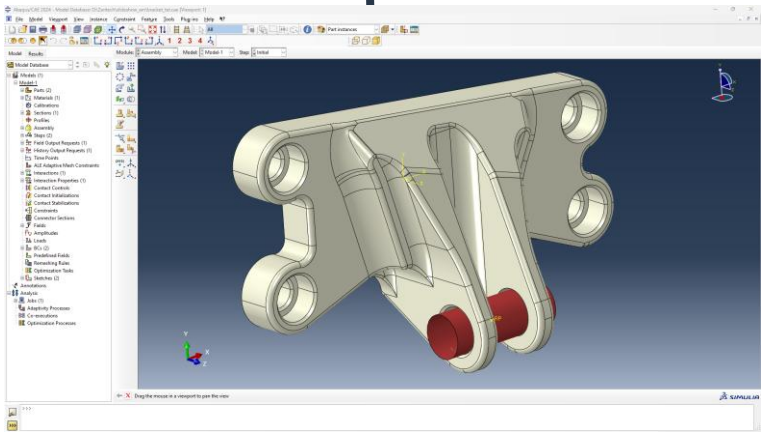

F.E. pre-processing

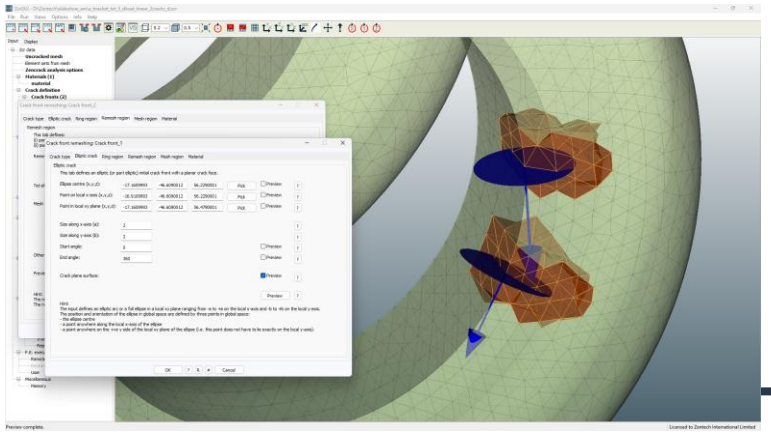

Zencrack pre-processing

USER INPUT
An existing f.e. mesh of an uncracked component

USER INPUT
Additional data e.g. crack location, size, growth law, load history

Analysis loop

ZENCRACK
Creates f.e. mesh of the initial cracked component

F.E. CODE
Analysis

ZENCRACK
Evaluates crack growth

ZENCRACK
Next f.e. analysis?

no

STOP

yes

ZENCRACK
Updates f.e. model

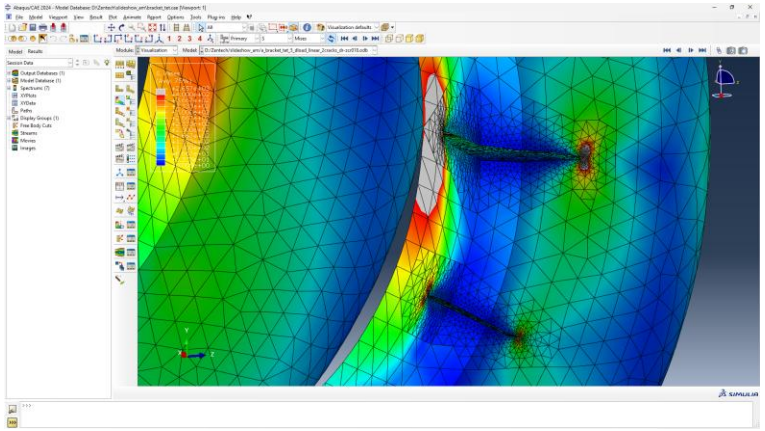

F.E. post-processing

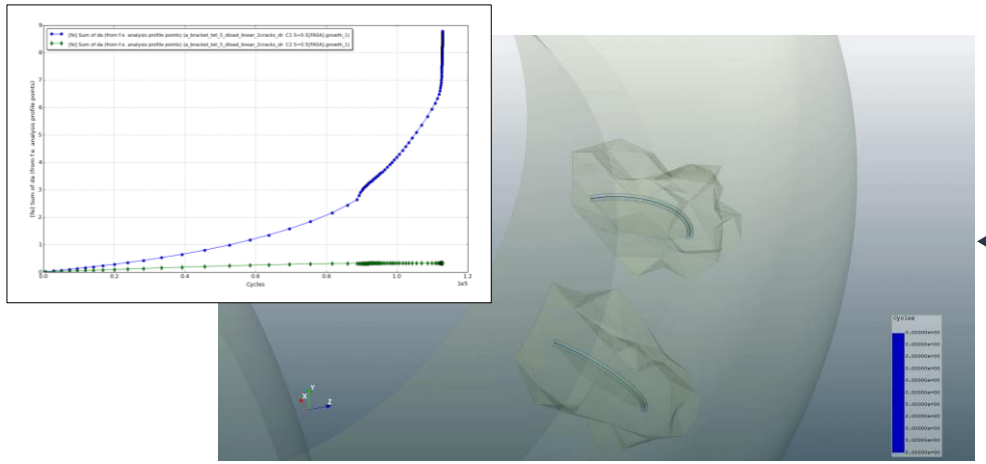

Zencrack post-processing

SIF solutions

- No SIF data exists in open literature for a semi-elliptic crack in a stud of an L-flange connection considering the actual 3D geometry of the threads
- To validate the 3D FEA approach, the M48 threaded rod geometry with length to minor diameter ratio of 1.65 was selected
  - SIF data has been reported by multiple authors for semi-elliptic crack shapes
  - To ensure consistency in the validation, an extra model with axisymmetric thread was required

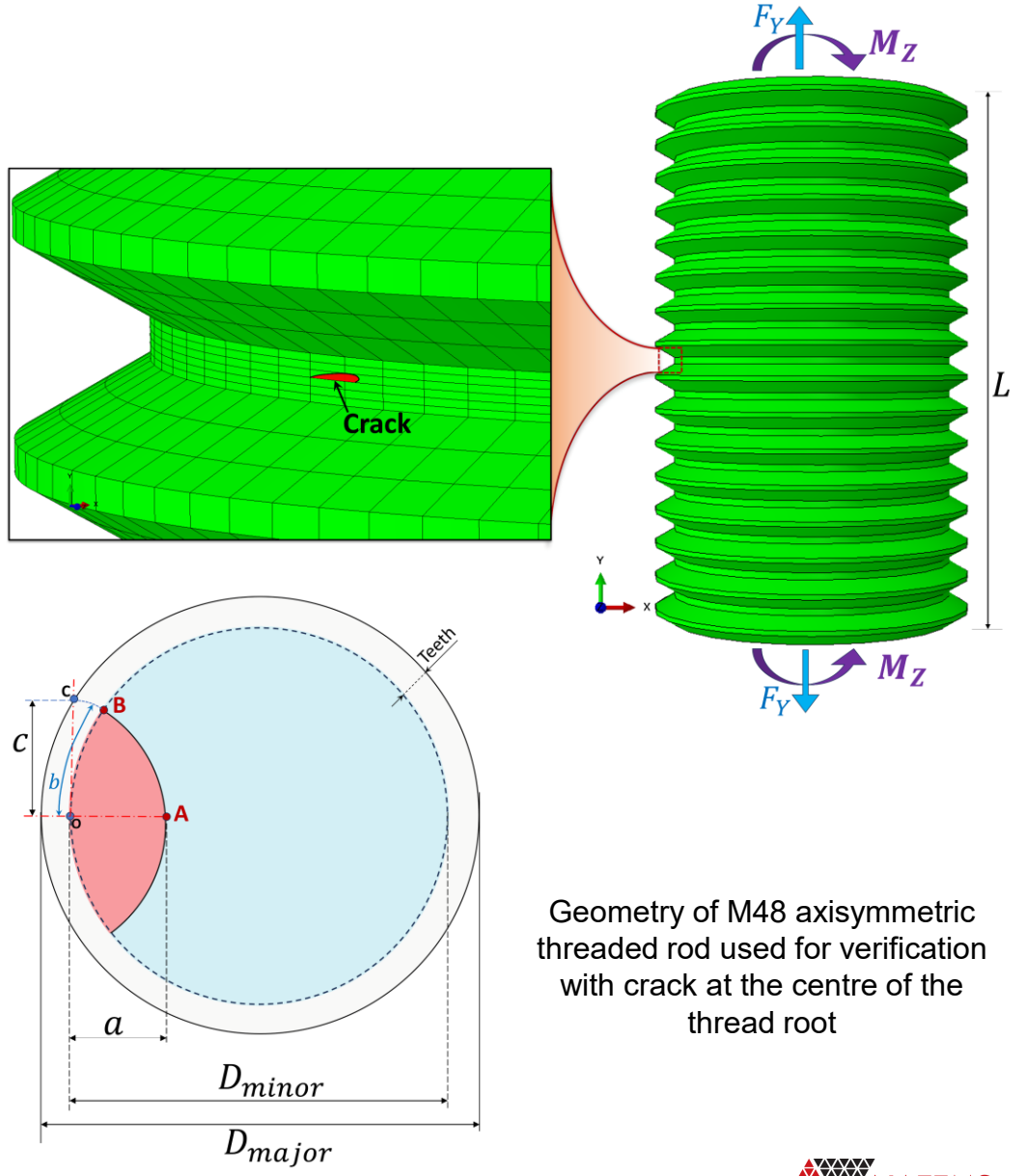

Geometry of M48 axisymmetric threaded rod used for verification with crack at the centre of the thread root

SIF solutions

- Good agreement with literature for this simplified case of axisymmetric thread and semi-elliptic crack

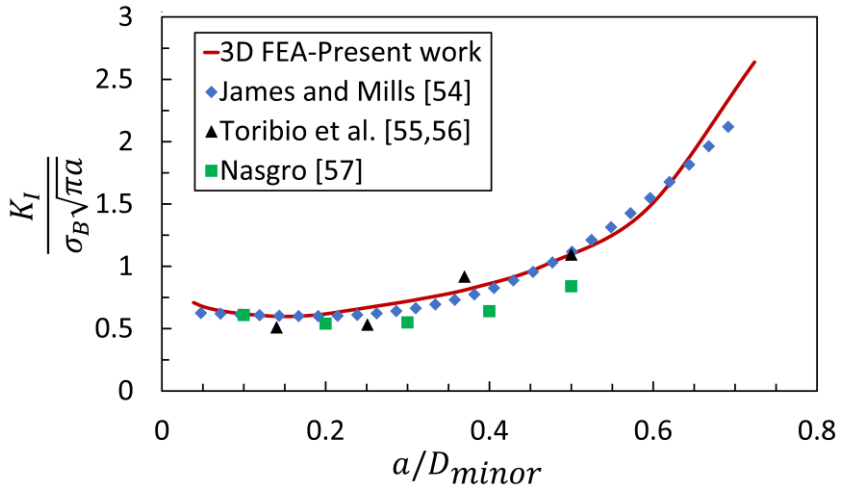

Comparison of SIF values for a semi-elliptic crack subjected to bending (deepest point of the crack) in axisymmetric thread

- The actual helix thread can then be compared with an axisymmetric thread
  - Crack shape allowed to develop naturally
  - For very short cracks with a/D less than about 0.05 the dimensionless SIF is nearly the same for axial and bending load
  - For short cracks with a/D less than about 0.25 the helix angle has little effect on the SIF
  - For large cracks neglecting the helix angle results in slightly increased SIF values

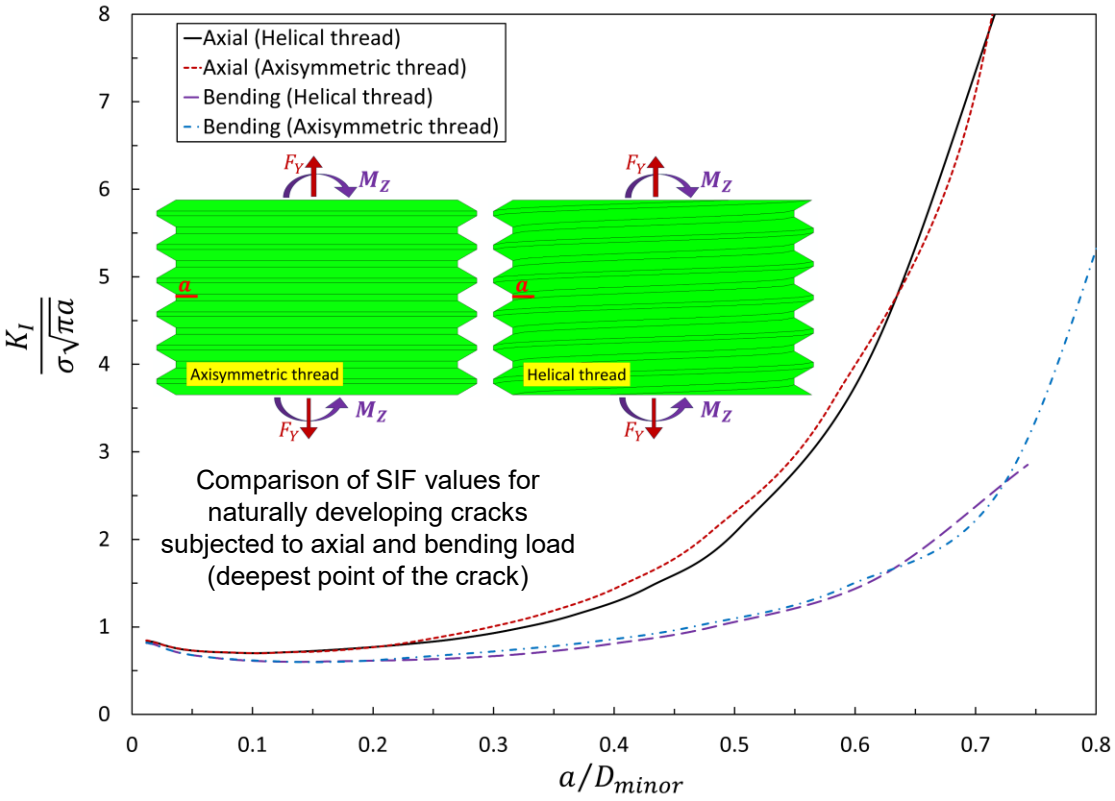

Comparison of SIF values for naturally developing cracks subjected to axial and bending load (deepest point of the crack)

SIF solutions

- The behavior in terms of crack shape development can also be considered
- Shown here for axisymmetric thread

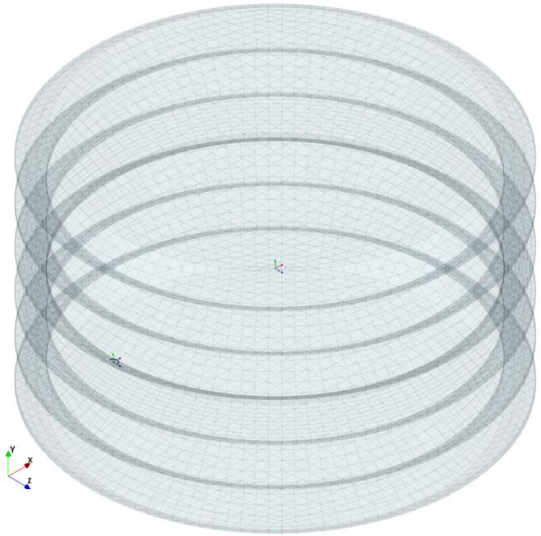

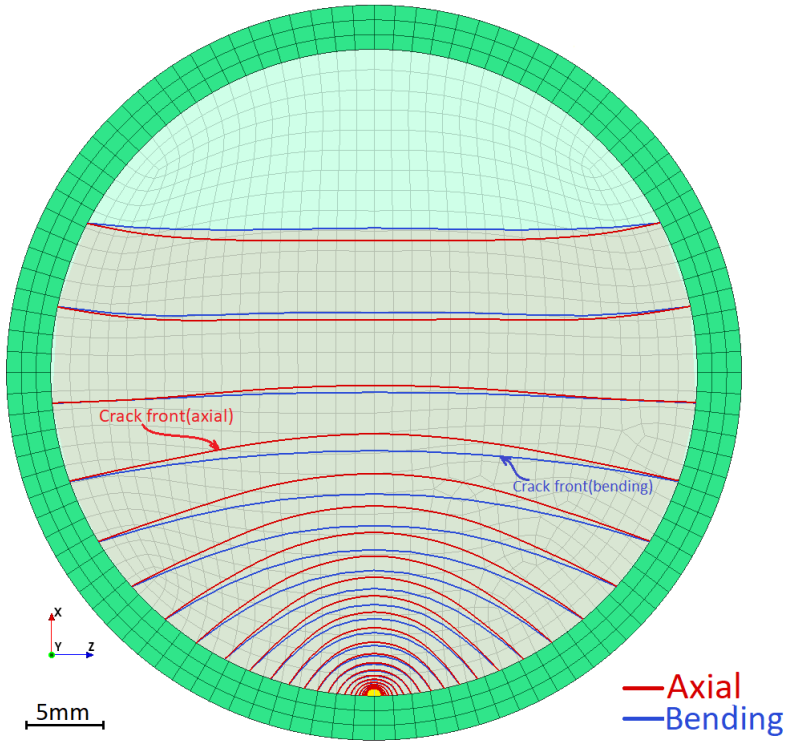

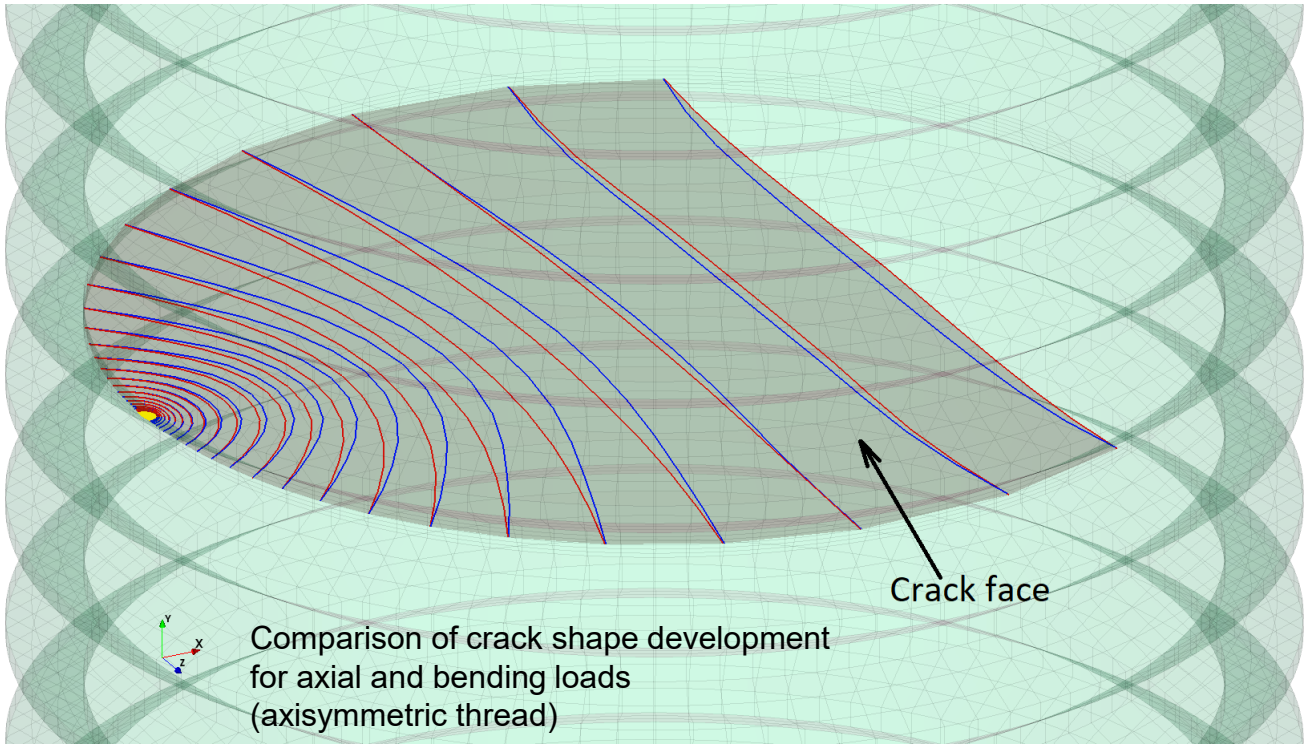

Comparison of crack shape development for axial and bending loads (axisymmetric thread)

SIF solutions

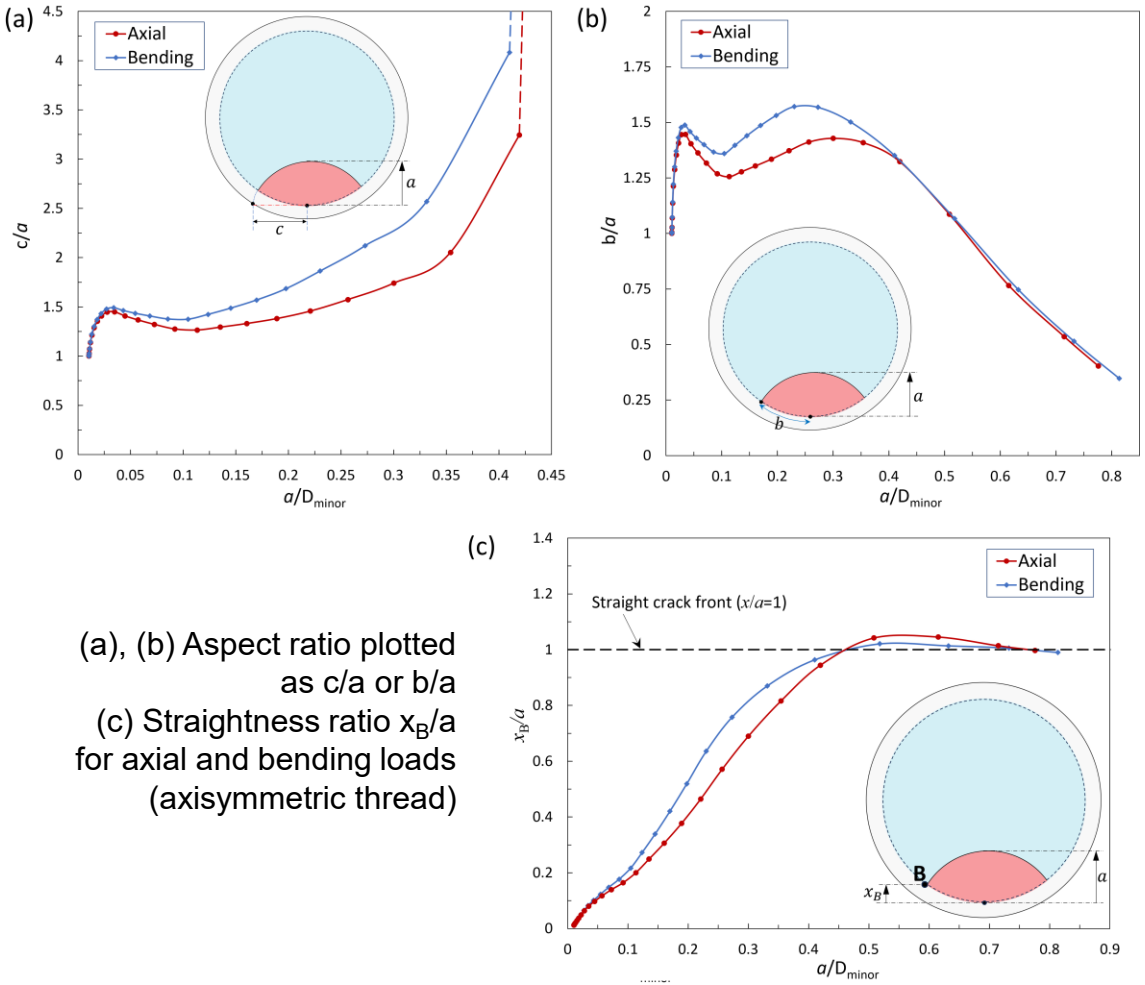

(a), (b) Aspect ratio plotted as c/a or b/a

(c) Straightness ratio x_B/a for axial and bending loads (axisymmetric thread)

Comparison of SIF at deepest point and surface point for for axial and bending loads (axisymmetric thread)

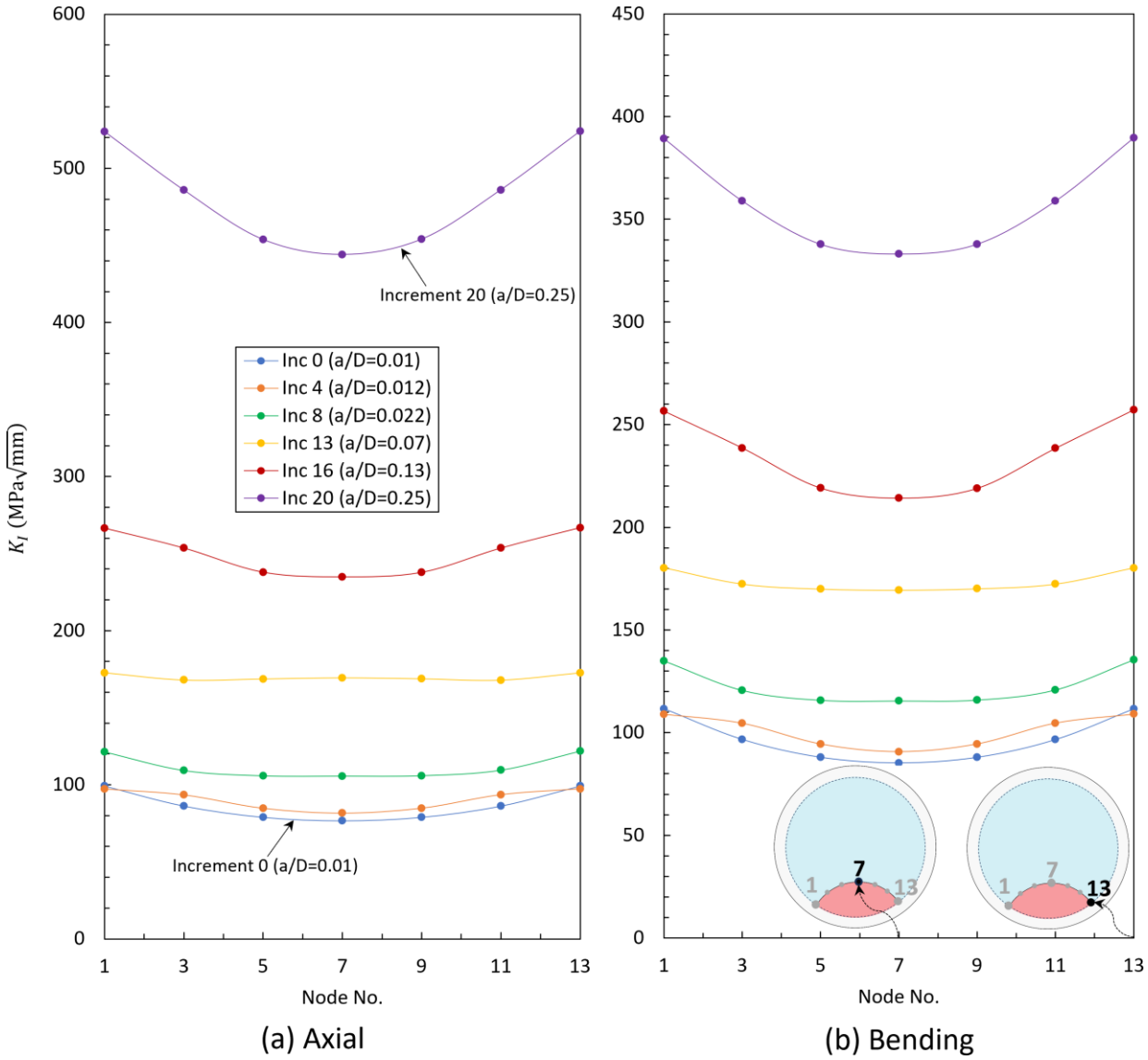

SIF solutions – parameterisation

Note: equations highlighted in red boxes are referenced on the final slide

- From these results it is possible to derive parametric SIF fits for helical and axisymmetric threads for initial crack a/c=1.0 and a=0.5mm
- Y_A and Y_B are geometry factors for axisymmetric thread (AT) and helical thread (HT):

$$K_I = (\sigma_A Y_A + \sigma_B Y_B)\sqrt{\pi a} \qquad \text{SIF at deepest point} \qquad (17)$$

where σ_A and σ_B represent stresses due to pure axial force and bending moment, respectively, and are obtained as follows:

$$\sigma_A = \frac{4F_Y}{\pi D_{minor}^2} \qquad (18)$$

$$\sigma_B = \frac{32M_Z}{\pi D_{minor}^3} \qquad (19)$$

$$Y_A^{AT} = \frac{1.232\left(\frac{a}{D_{minor}}\right)^2 + 0.01487\left(\frac{a}{D_{minor}}\right) + 0.1356}{\left(\frac{a}{D_{minor}}\right)^3 - 1.978\left(\frac{a}{D_{minor}}\right)^2 + 0.8268\left(\frac{a}{D_{minor}}\right) + 0.1516} \qquad (20)$$

$$Y_A^{HT} = \frac{-0.01435\left(\frac{a}{D_{minor}}\right)^2 + 0.1373\left(\frac{a}{D_{minor}}\right) + 0.04894}{\left(\frac{a}{D_{minor}}\right)^3 - 1.463\left(\frac{a}{D_{minor}}\right)^2 + 0.4833\left(\frac{a}{D_{minor}}\right) + 0.05438} \qquad (22)$$

$$Y_B^{AT} = \frac{-0.2996\left(\frac{a}{D_{minor}}\right)^2 + 0.3268\left(\frac{a}{D_{minor}}\right) + 0.03324}{\left(\frac{a}{D_{minor}}\right)^3 - 1.871\left(\frac{a}{D_{minor}}\right)^2 + 0.8411\left(\frac{a}{D_{minor}}\right) + 0.0349} \qquad (21)$$

$$Y_B^{HT} = \frac{-0.0369\left(\frac{a}{D_{minor}}\right)^2 + 0.3027\left(\frac{a}{D_{minor}}\right) + 0.07709}{\left(\frac{a}{D_{minor}}\right)^3 - 2.195\left(\frac{a}{D_{minor}}\right)^2 + 1.097\left(\frac{a}{D_{minor}}\right) + 0.08538} \qquad (23)$$

$$0.01 \leq a \Big/ D_{minor} \leq 0.75$$

Mesh examples

- The next slides give animation examples of how the remeshing process operates for these types of thread models for a bending load case
- First an axisymmetric thread, followed by a helical thread

Axisymmetric thread

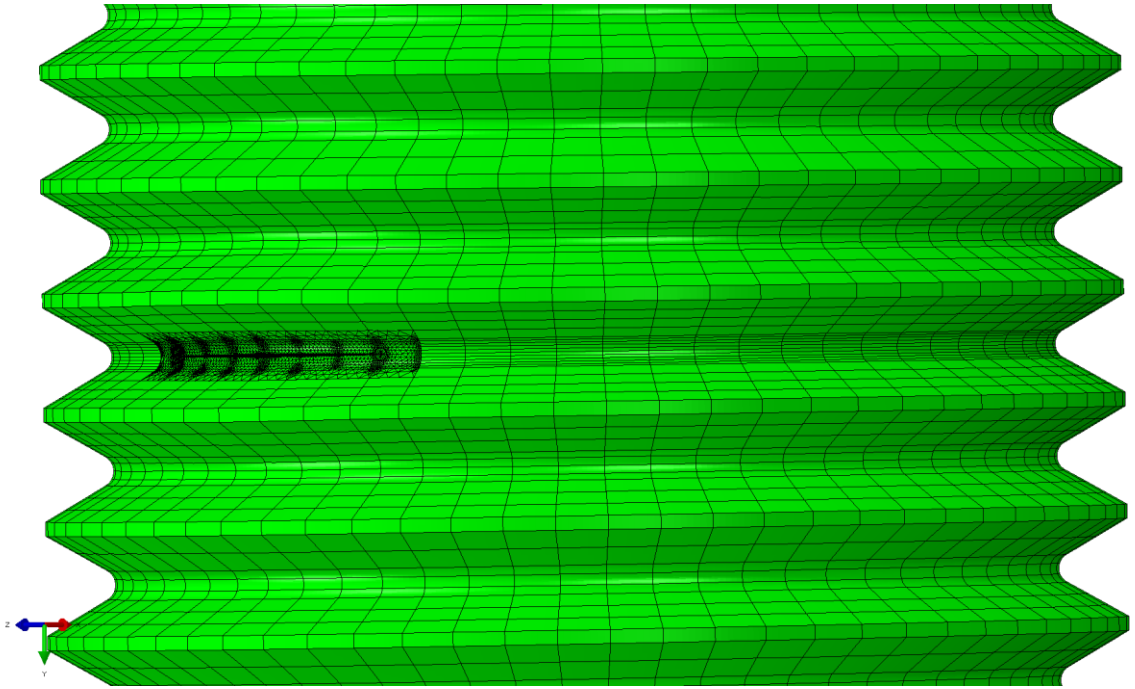

Helical thread

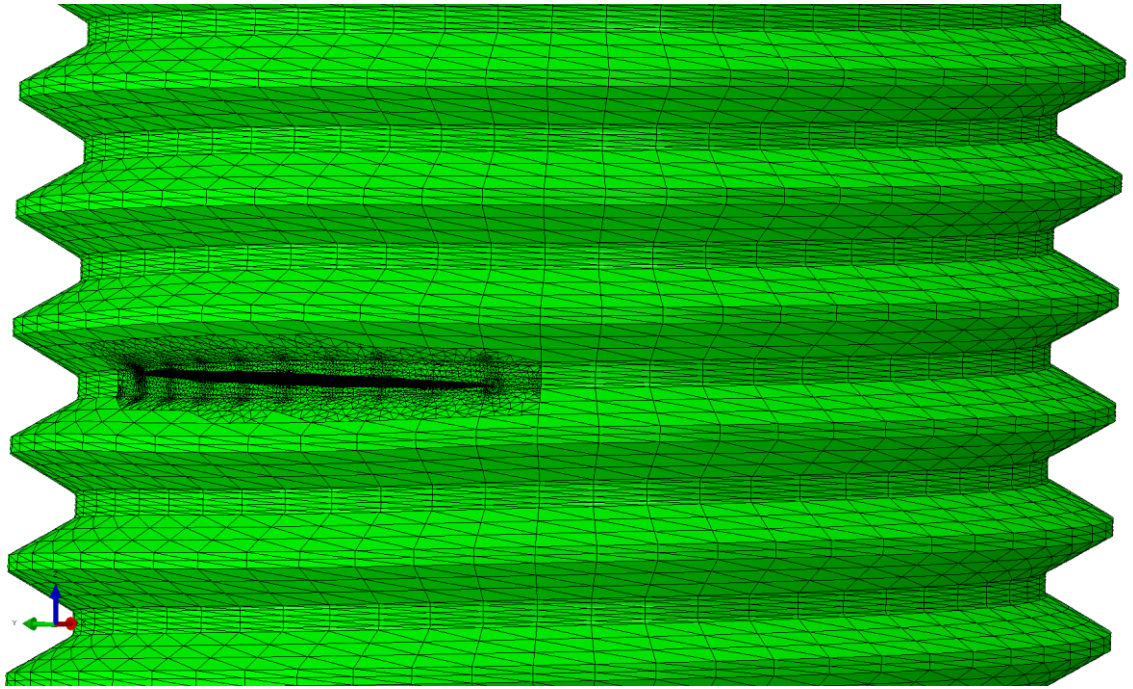

Axisymmetric thread

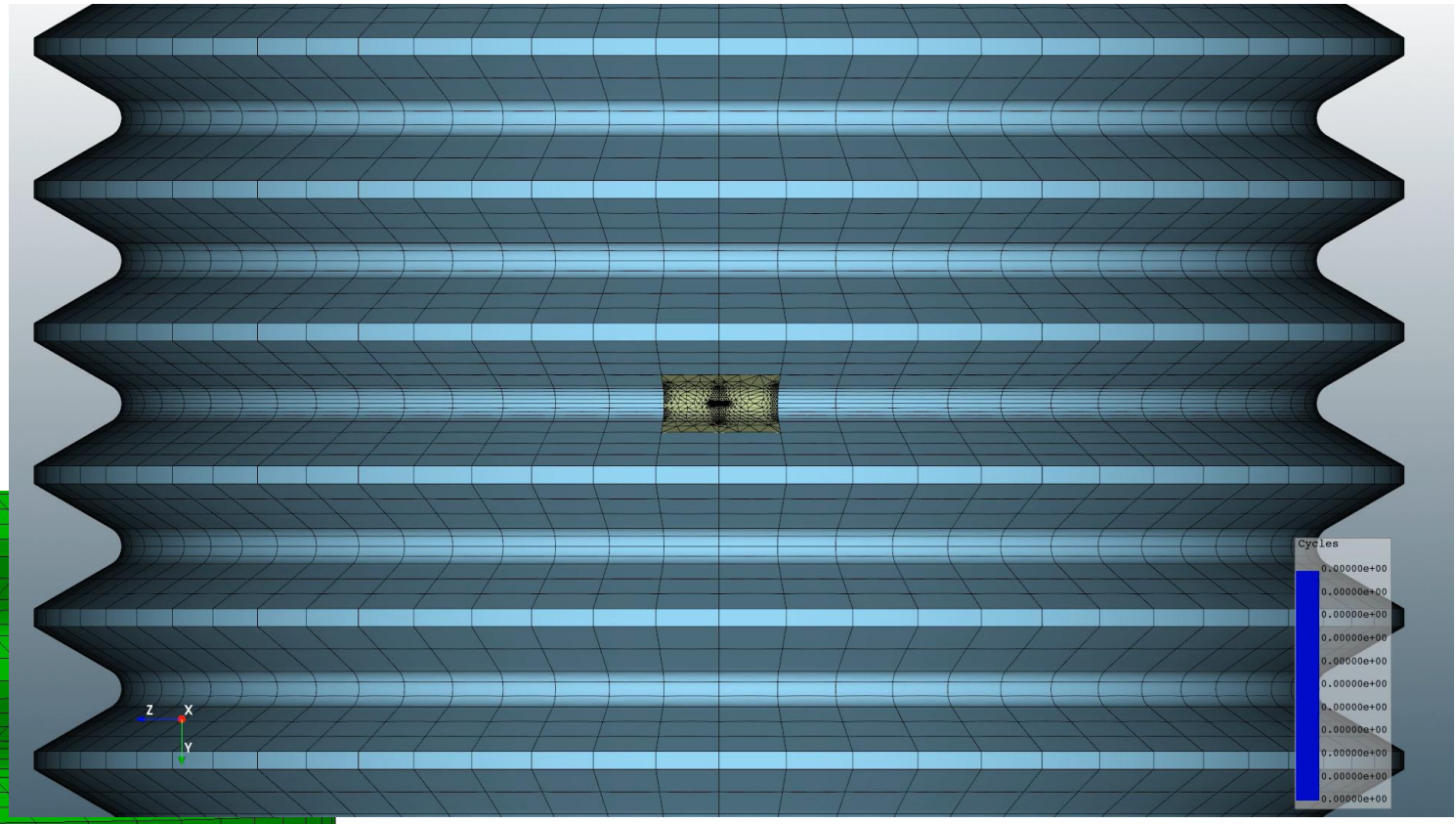

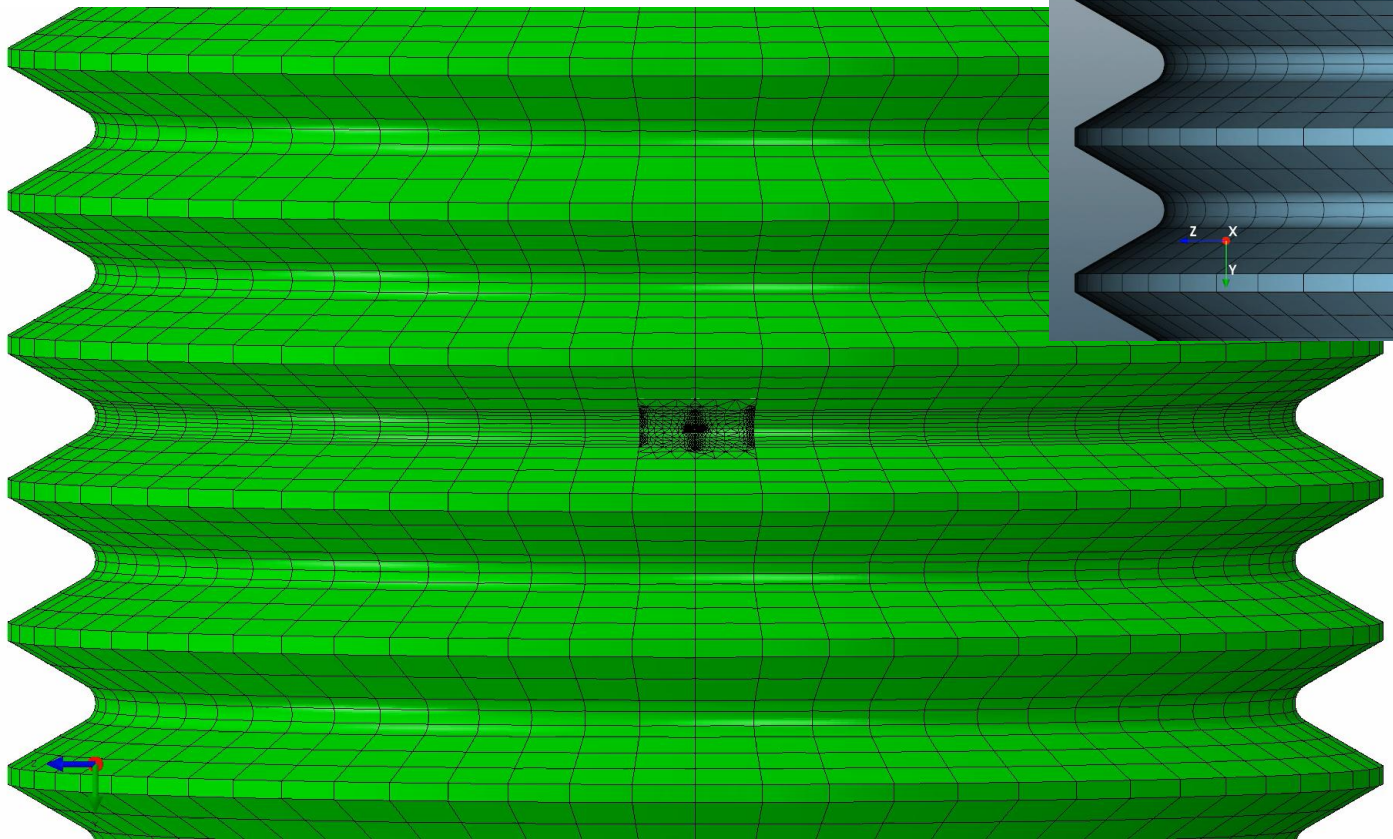

Helical thread

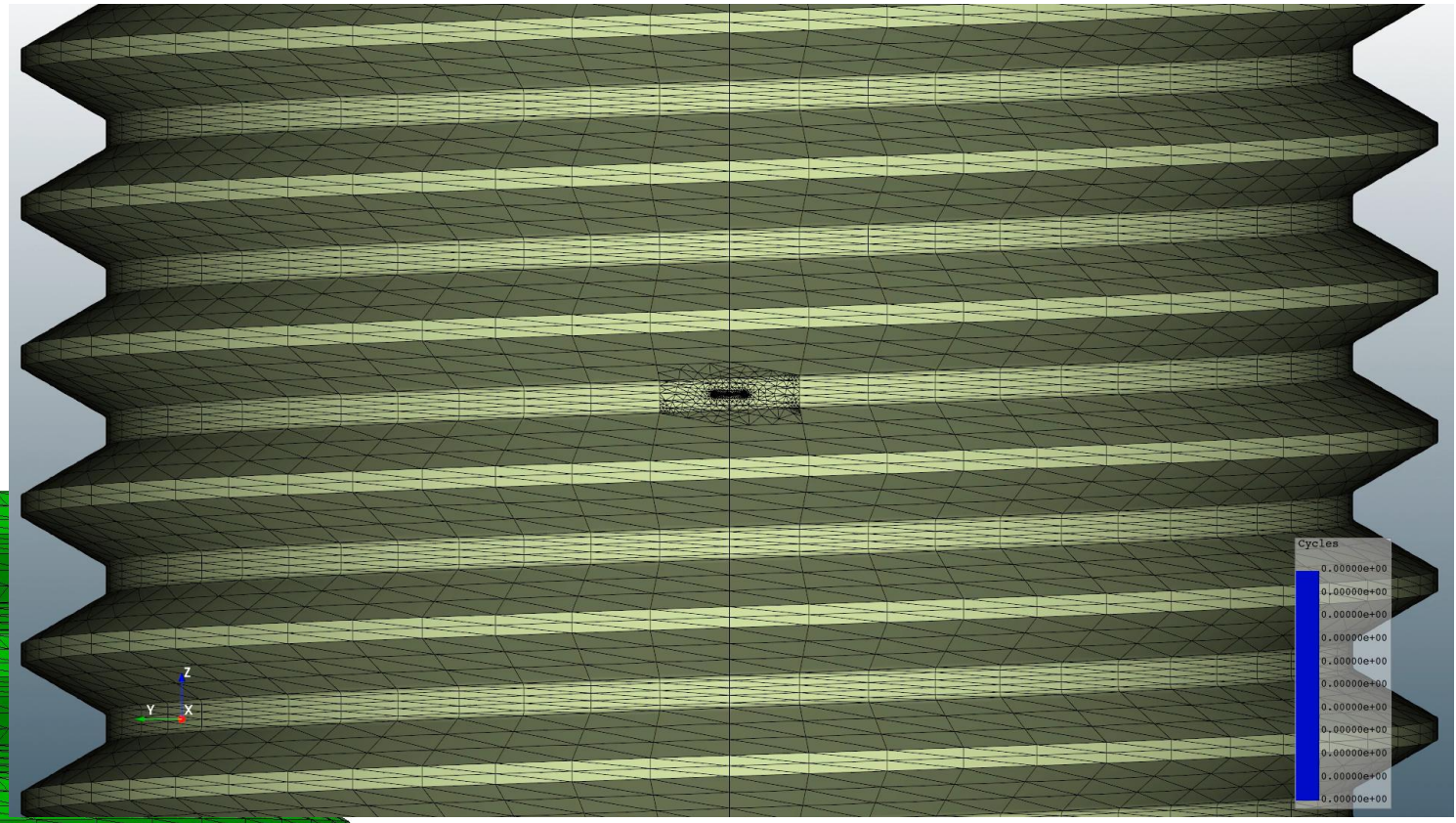

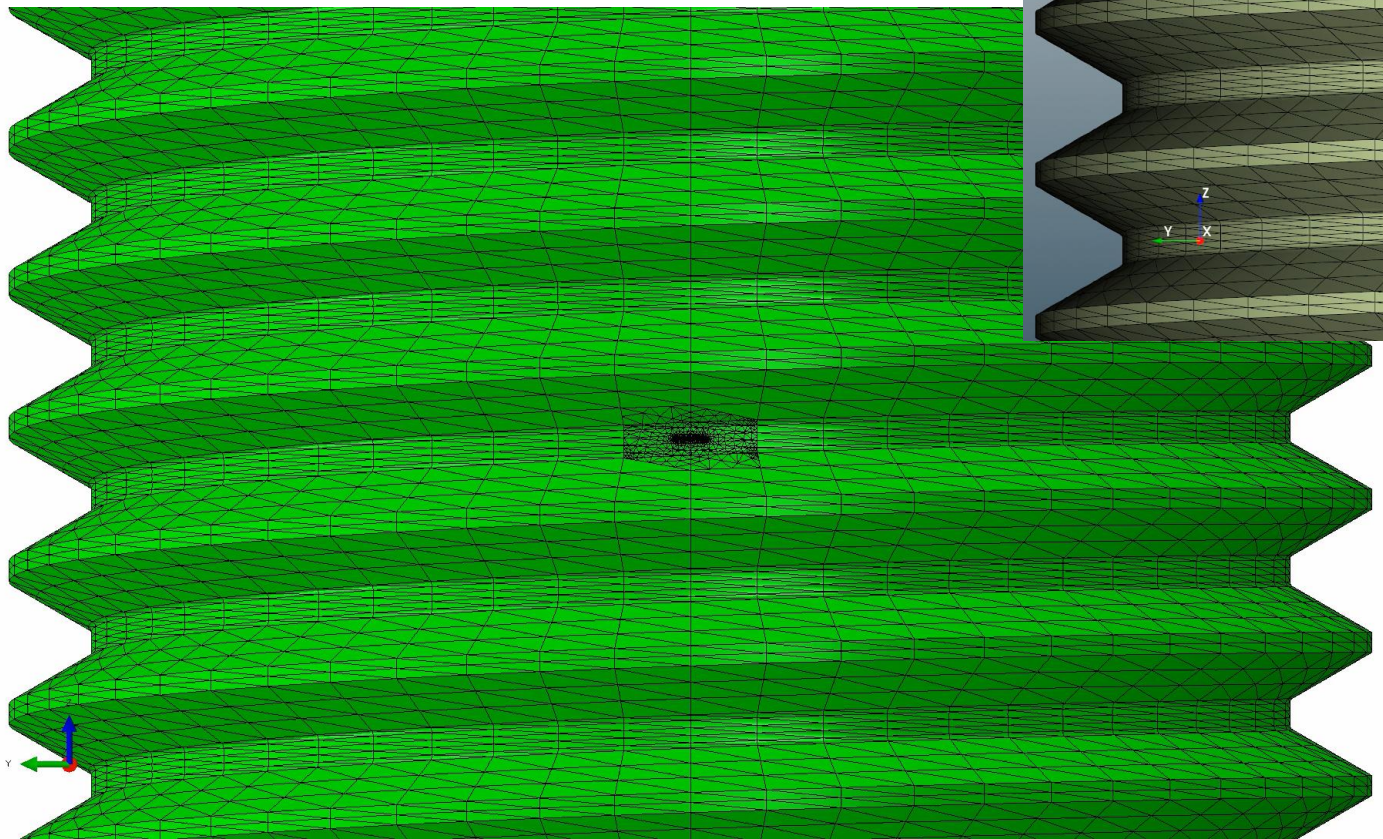

Preload simulation

- Assess uncracked and cracked studs
  - Global-submodel approach for cracked studs
- Analysis steps:
  - Step 1 – preload by turn-of-nut
  - Step 2 – application of external load to top flange with bottom flange fixed

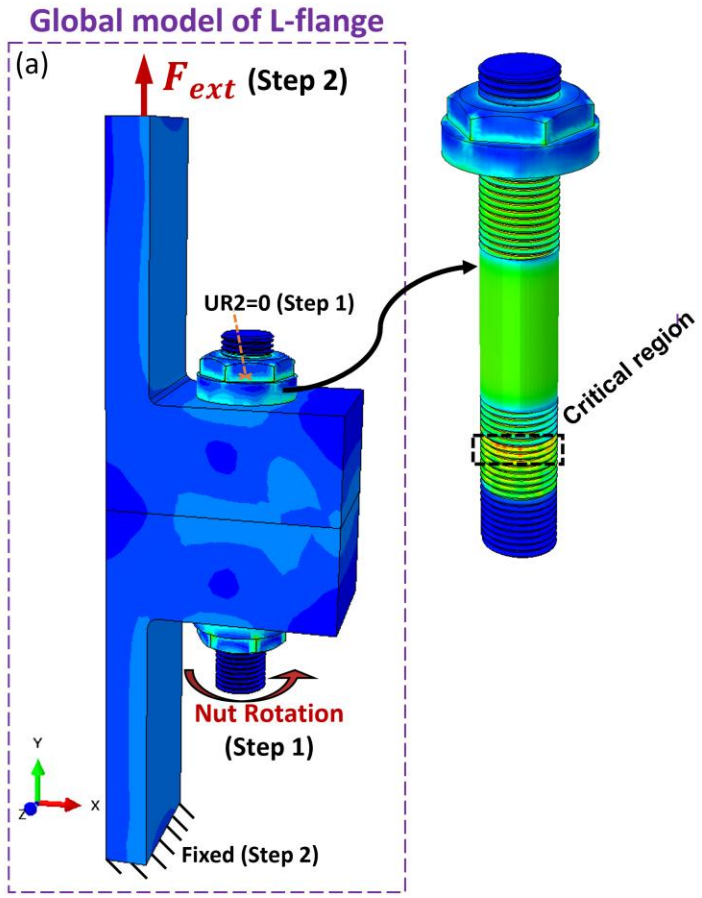

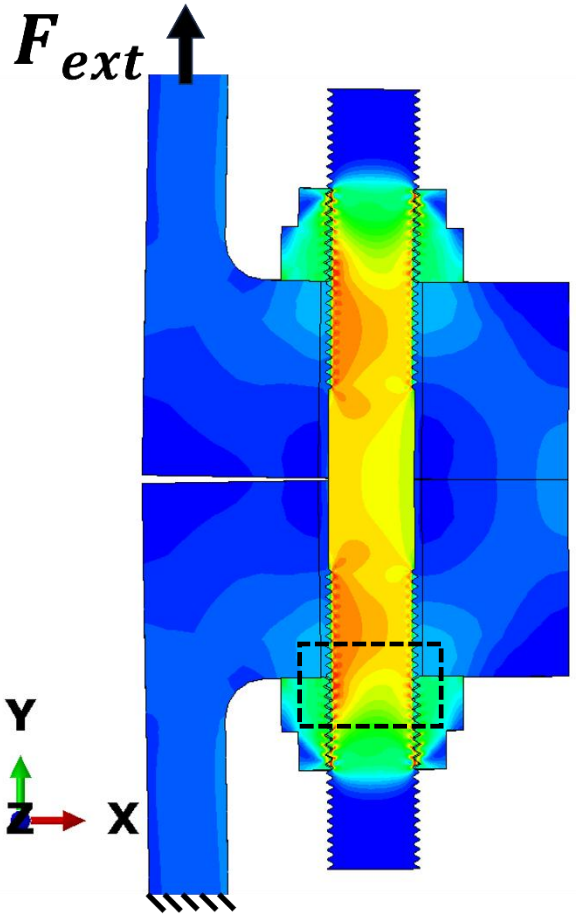

Preload simulation

- Zencrack analysis for crack shape development via Paris law in submodel
  - Allows extraction of SIF data
- Manual integration process using a NASGRO law with the extracted SIFs to calculate fatigue life

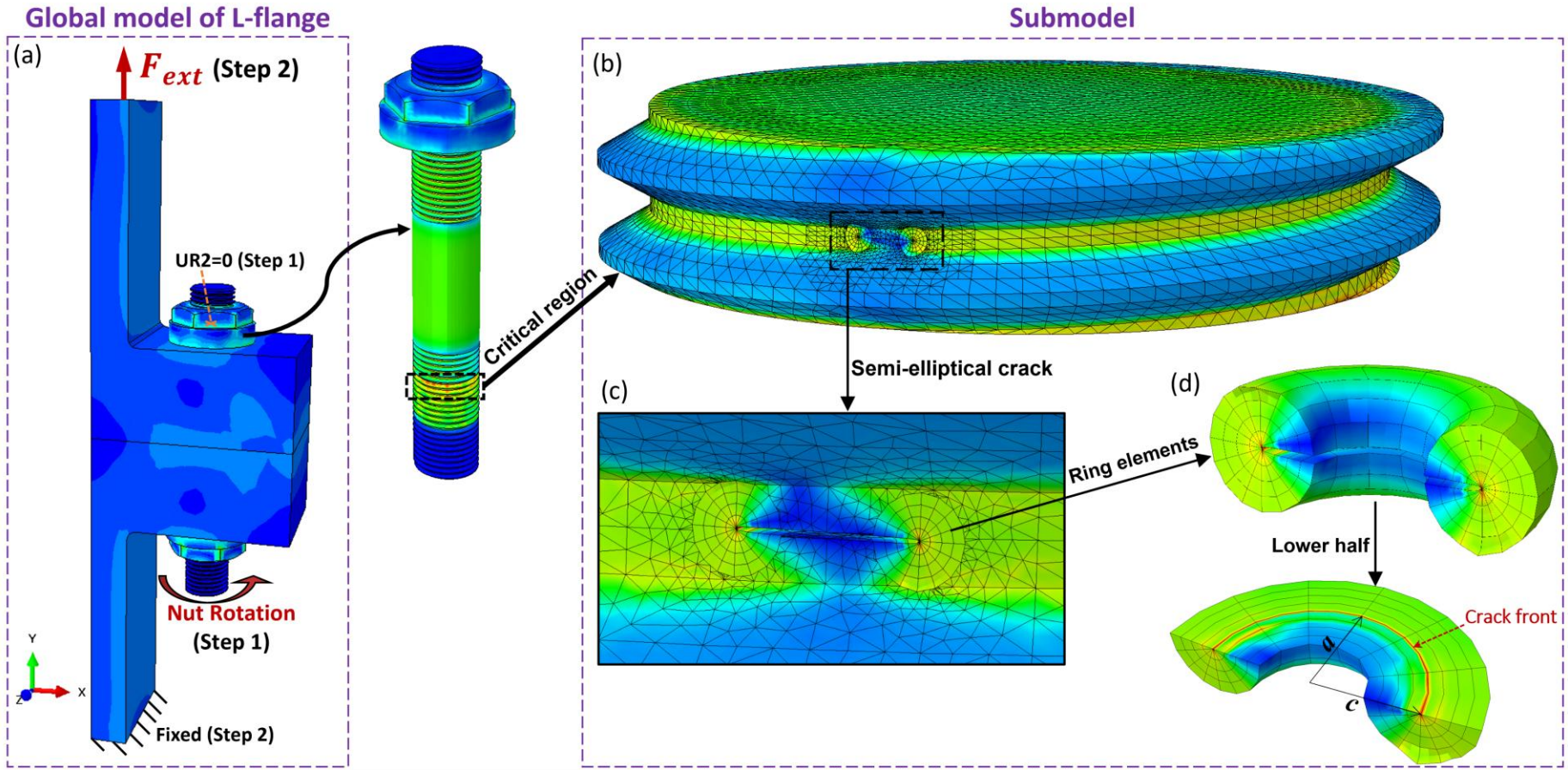

Global model: Abaqus/Explicit
Submodel: Abaqus/Standard

Preload simulation

- Nut rotation to generate bolt preload

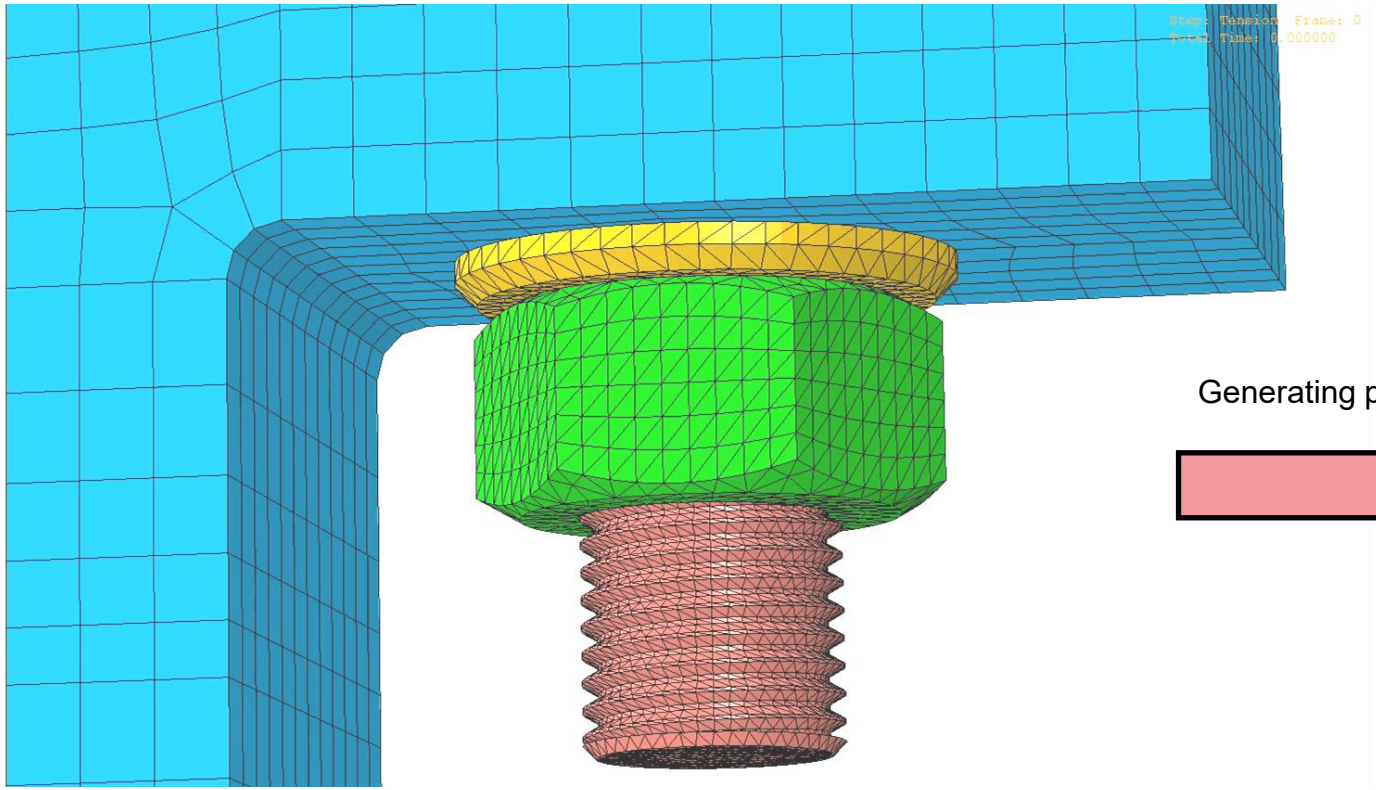

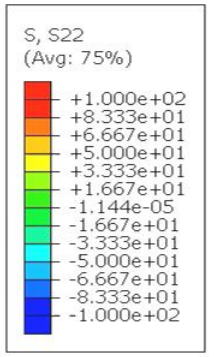

Generating preload

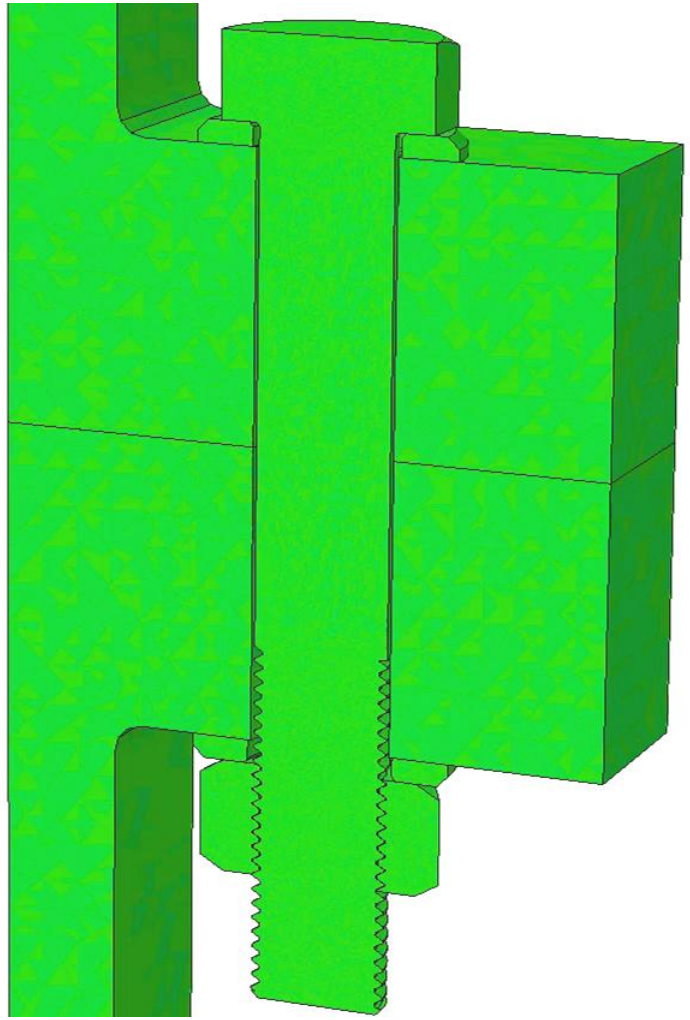

Preload simulation – fatigue life

- Cyclic external load with stress ratio R=0
- Nasgro equation

$$\frac{da}{dN} = g(a) = C\left[\left(\frac{1-\gamma}{1-R_B}\right)\Delta K\right]^n \frac{\left(1-\frac{\Delta K_{I,th}}{\Delta K_I}\right)^p}{\left(1-\frac{K_{I,max}}{K_C}\right)^q} \quad (6)$$

- Integration using this equation and SIF results from the FEA to calculate cycles to failure

$$N_f = \int_{a_i}^{a_c} \frac{1}{g(a)}\,da \approx \frac{a_c - a_i}{2k} \sum_{j=i+1}^{k} \left(\frac{1}{g(a_{j-1})} + \frac{1}{g(a_j)}\right) \quad (14)$$

- Generation of S-N curve of form

$$N_f = A(\Delta S^{nom})^{-m} \quad (15)$$

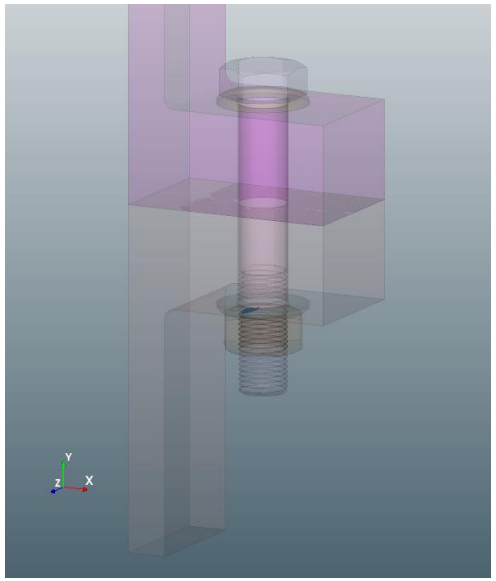

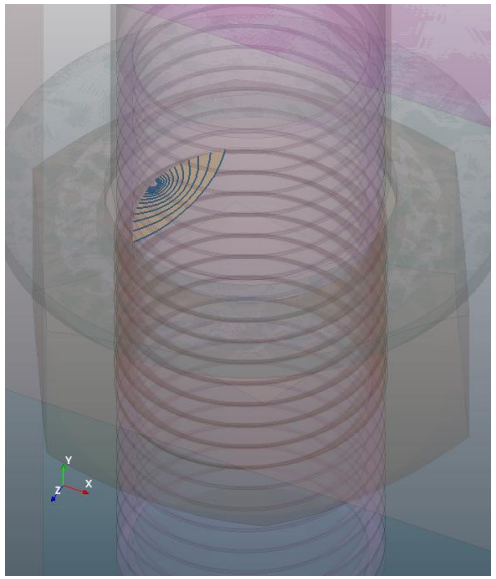

Crack profiles calculated in the submodel analysis superimposed onto the global model

Preload experiment and FEA comparison

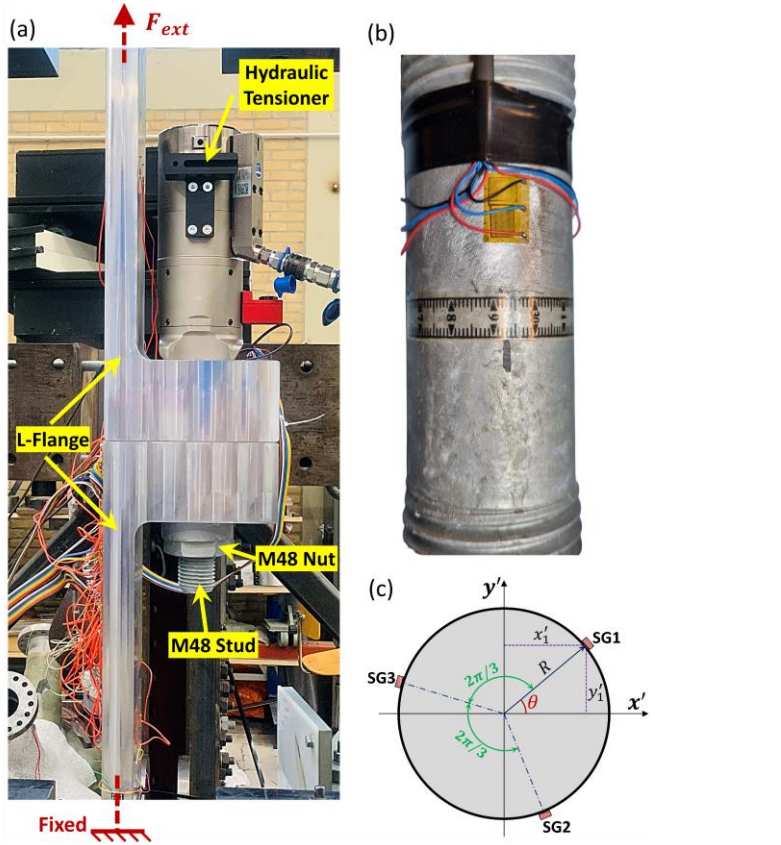

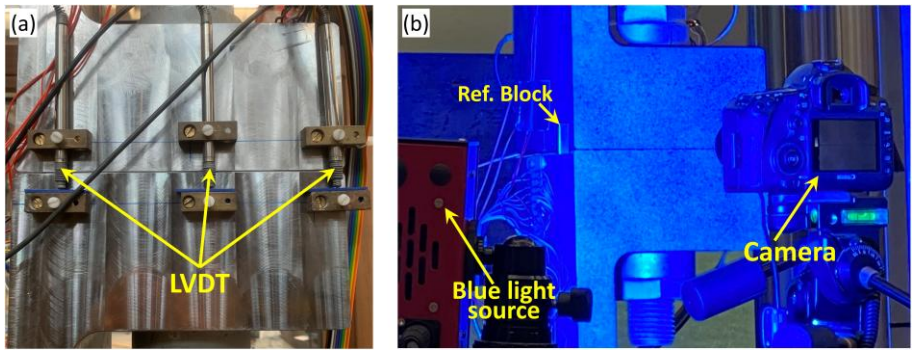

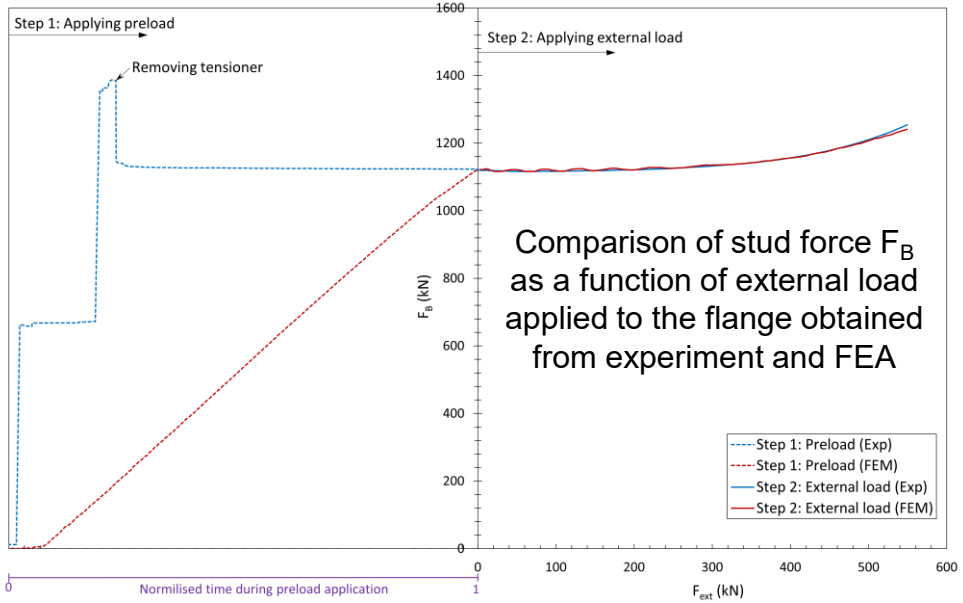

Comparison of stud force F_B as a function of external load applied to the flange obtained from experiment and FEA

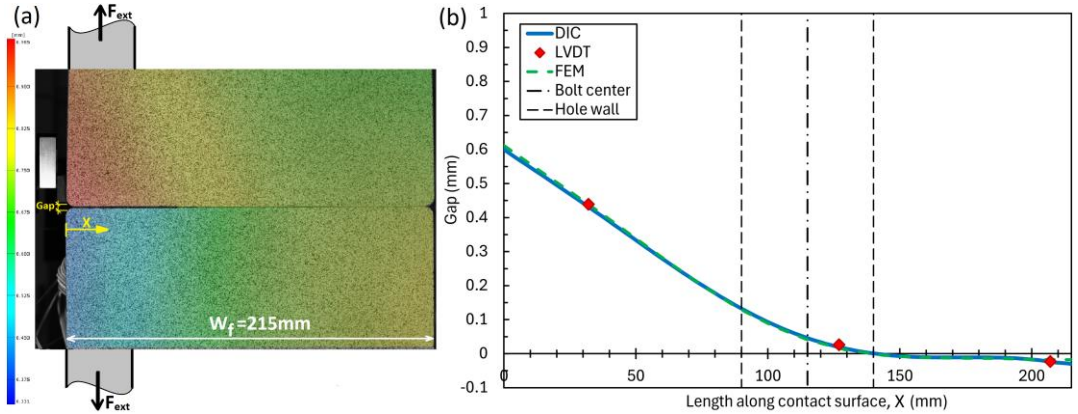

Distribution of vertical flange displacement from DIC analysis and comparison of flange gap from DIC, LVDT and FEA

LVDT = linear variable differential transformer
DIC = digital image correlation

Effect of preload on LTF

- The stud force and preload level is determined from the FEA as a function of nut rotation
- By applying different nut rotation, the effect of different preload levels can be investigated

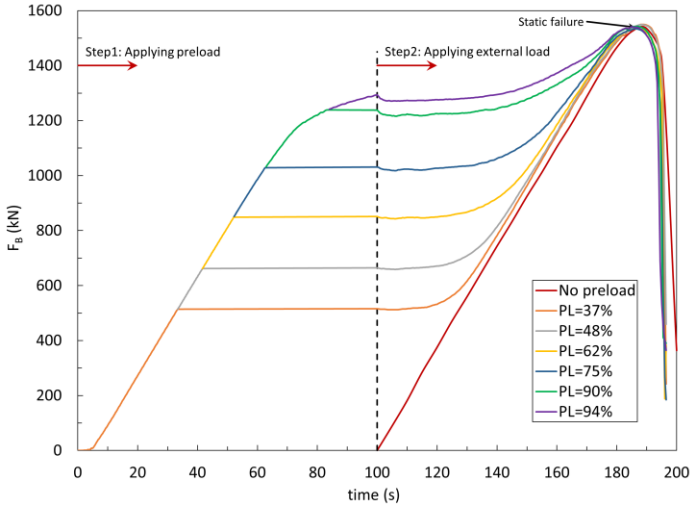

Stud force during different preload and external load applications for different preload levels

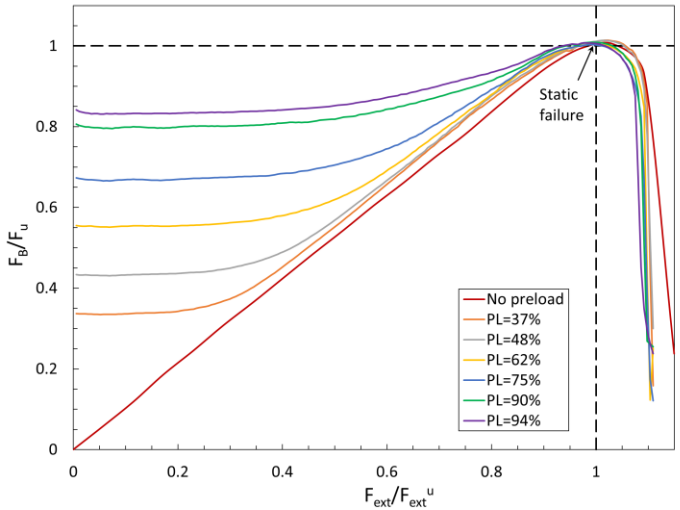

Variation of stud force with external load for different preload levels

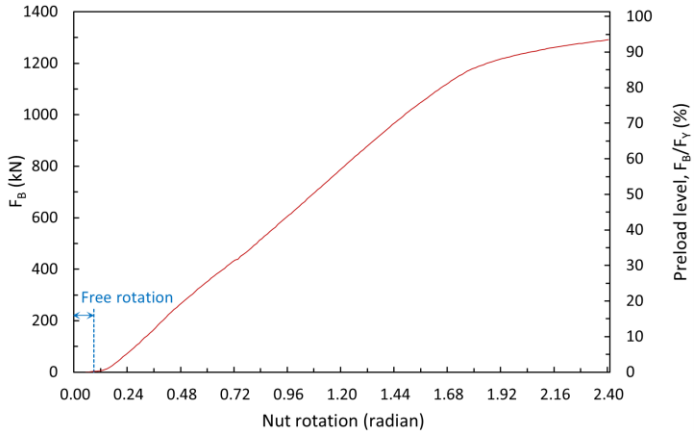

Stud force and preload as a function of nut rotation

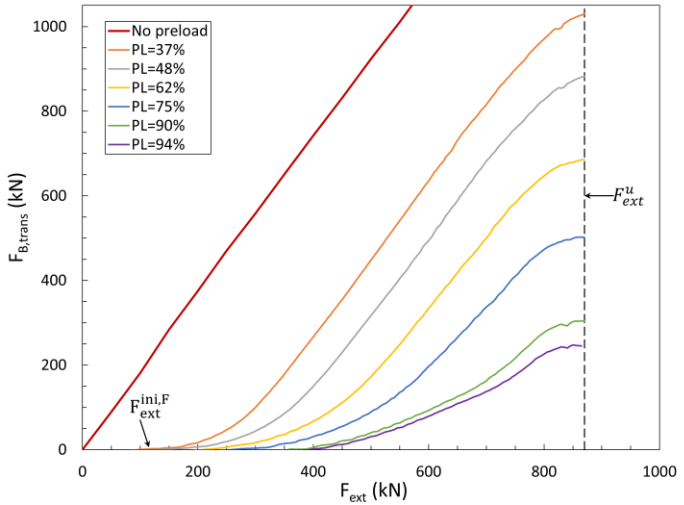

Portion of external load transferred to stud as function of external load

Effect of preload on LTF - parameterisation

Required external load for initiation of load transfer to the stud as a function of preload and stud force at various preload levels:

$$\frac{F_{ext}^{ini,F}}{F_{PL}} = \left(\frac{F_{PL}}{F_y}\right)\left[0.4682 + 1.232\left(\frac{F_{PL}}{F_y}\right) - 3.395\left(\frac{F_{PL}}{F_y}\right)^2 + 2.062\left(\frac{F_{PL}}{F_y}\right)^3\right] \quad (27)$$

$$\begin{cases} \frac{F_B}{F_{PL}} = 1 + \left(\frac{F_{ext} - F_{ext}^{ini,F}}{F_u}\right)^2 \left[B_1\left(\frac{F_{ext} - F_{ext}^{ini,F}}{F_u}\right)^2 + B_2\left(\frac{F_{ext} - F_{ext}^{ini,F}}{F_u}\right) + B_3\right] & F_{ext} \geq F_{ext}^{ini,F} \\ \frac{F_B}{F_{PL}} = 1 & F_{ext} \leq F_{ext}^{ini,F} \end{cases} \quad (28)$$

Variation of stud moment around z-axis with external load as a function of preload:

$$\frac{F_{ext}^{ini,M}}{F_{PL}} = \left(\frac{F_{PL}}{F_y}\right)\left[1.206 - 6.415\left(\frac{F_{PL}}{F_y}\right) + 19.2\left(\frac{F_{PL}}{F_y}\right)^2 - 24.76\left(\frac{F_{PL}}{F_y}\right)^3 + 11.07\left(\frac{F_{PL}}{F_y}\right)^4\right] \quad (30)$$

$$\begin{cases} \frac{M_{Z,B}}{F_{ext}^u \times d_{ecc}} = \frac{\left(\frac{F_{ext} - F_{ext}^{ini,M}}{F_u}\right)}{C_1\left(\frac{F_{ext} - F_{ext}^{ini,M}}{F_u}\right)^3 + C_2\left(\frac{F_{ext} - F_{ext}^{ini,M}}{F_u}\right)^2 + C_3\left(\frac{F_{ext} - F_{ext}^{ini,M}}{F_u}\right) + C_4} & F_{ext} \geq F_{ext}^{ini,M} \\ M_{Z,B} = 0 & F_{ext} \leq F_{ext}^{ini,M} \end{cases} \quad (29)$$

Coefficients B_n and C_n are functions of preload

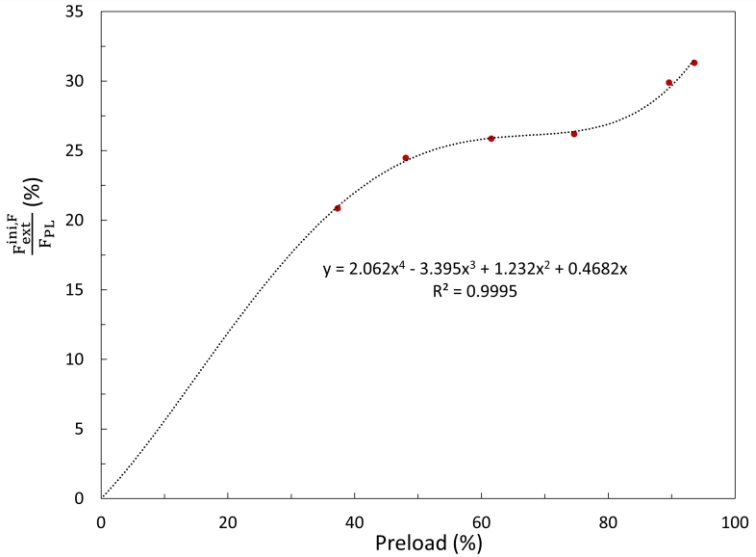

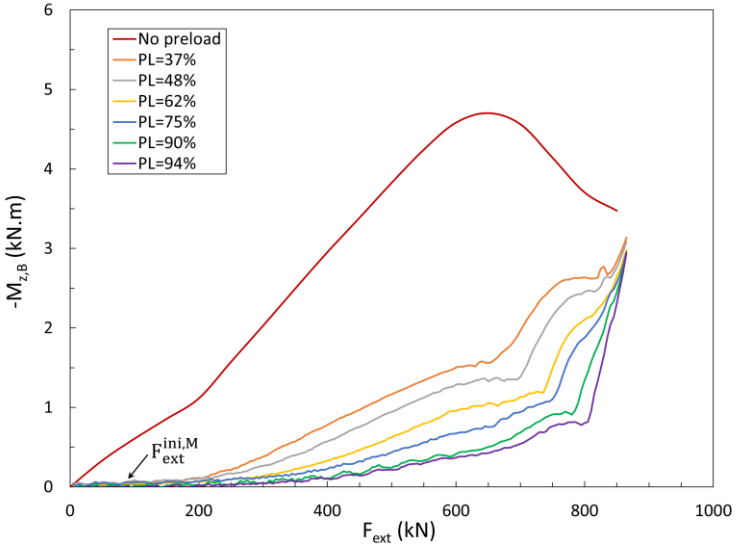

Effect of preload on SIF - parameterisation

Similar to the definitions used earlier for the bolt under axial and bending load, geometry factors can be defined for the flange connection:

$$Y_A = \frac{1}{\left(1 - \frac{a}{D_{minor}}\right)^{3/2}} \left[\frac{0.05124\left(\frac{a}{D_{minor}}\right) + 0.001077}{\left(\frac{a}{D_{minor}}\right)^2 - 0.002986\left(\frac{a}{D_{minor}}\right) + 0.00192} \right] \qquad 0.02 \leq a \Big/ D_{minor} \leq 0.3 \qquad (32)$$

$$Y_B = \frac{1}{\left(1 - \frac{a}{D_{minor}}\right)^{3/2}} \left[\frac{0.0003131\left(\frac{a}{D_{minor}}\right) + 0.00001949}{\left(\frac{a}{D_{minor}}\right)^3 - 0.2002\left(\frac{a}{D_{minor}}\right)^2 + 0.0173\left(\frac{a}{D_{minor}}\right) - 0.0002349} \right] \qquad (33)$$

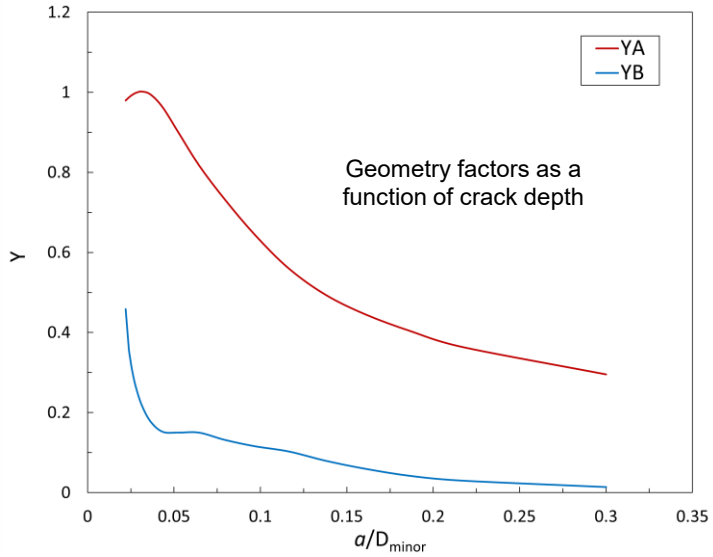

This allows SIF to be determined for different combinations of preload and external load.

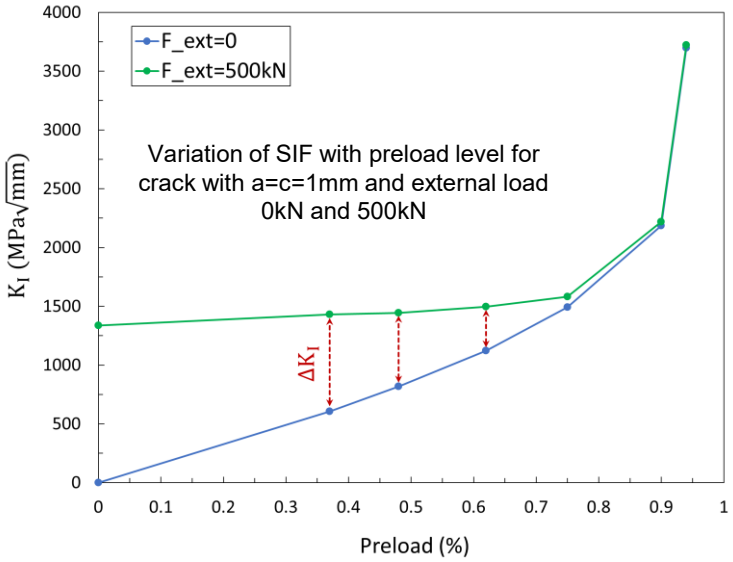

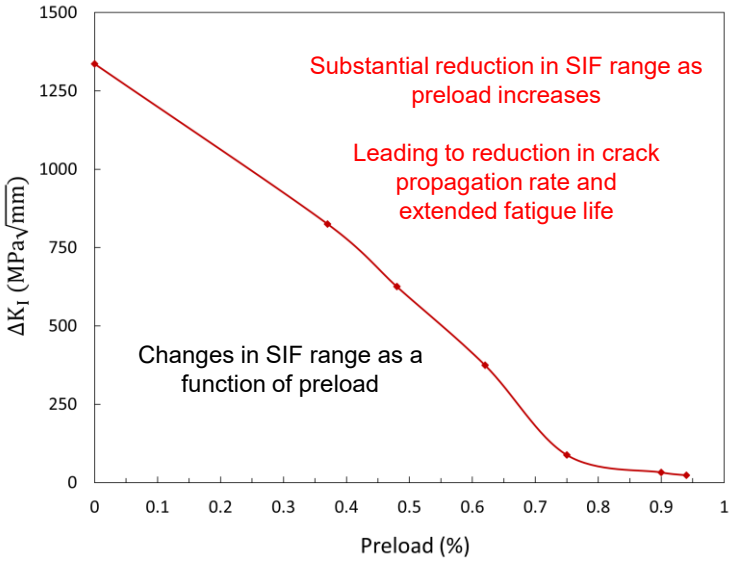

Effect of preload on fatigue life

Based on these parameterised results, S-N curves for different preload levels can be generated following a sequence of steps:

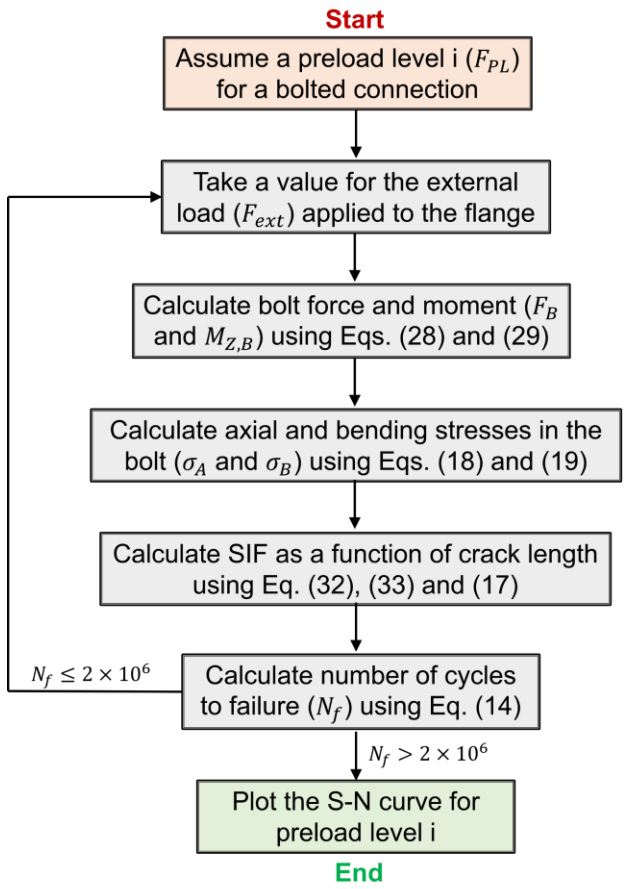

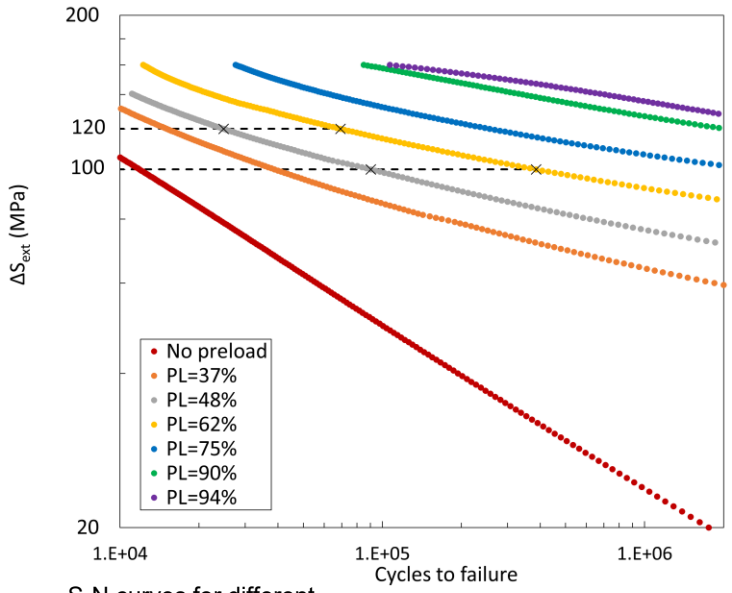

S-N curves for different preload levels based on external stress range applied to the tower shell

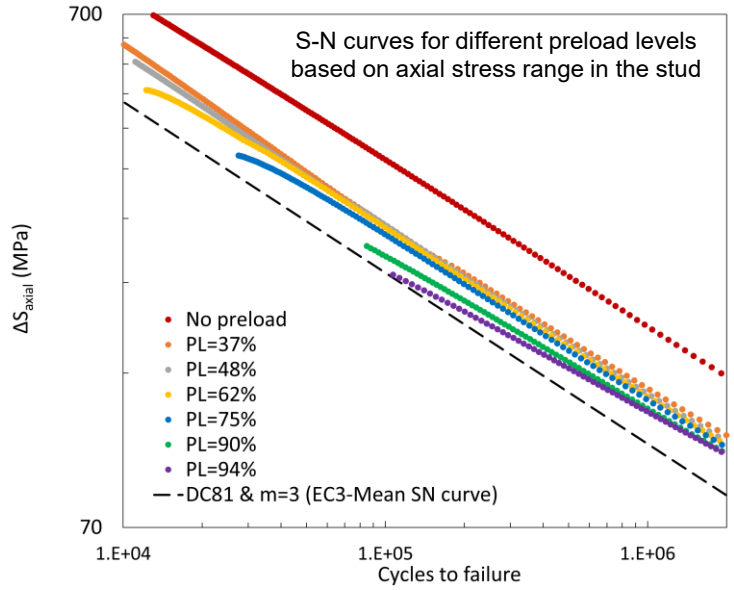

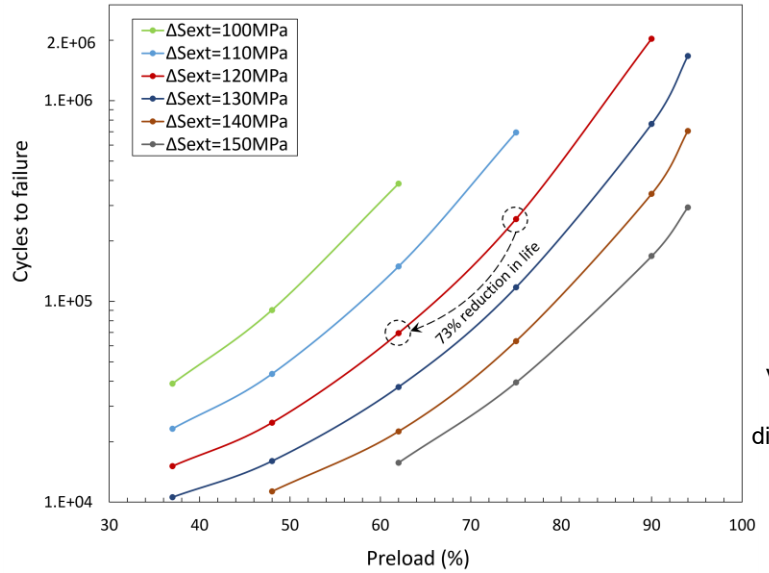

Variation of fatigue life as a function of preload for different external stress range applied to the tower shell

Conclusions

- Advanced FEA modelling including fatigue crack growth simulation and complex contact interactions has enabled generation of parameterised equations related to stress intensity factors and load transfer function as a function of axial and bending load
  - This enables more precise calculation of fatigue life than previously possible
  - In turn, this reduces design conservatism
- The strong influence of preload loss on fatigue life highlights the need for accurate maintenance strategies to allow in-service preload levels to be maintained
- Validation of SIF calculation from FEA for bolt models has been demonstrated for simplified axisymmetric thread and semi-elliptic cracks using existing published data
  - Solutions for realistic threads and crack shape development, not previously available in open literature, have been generated
- Validation of preload FEA has been demonstrated via experimental tests

Further work and limitations

- Flange geometry was idealized and potential geometric imperfections ignored
- The analysis considered a single crack position at the peak stress location in the thread
  - Distributed thread damage was not considered
- The same initial crack size was considered throughout, but manufacturing processes may generate alternative initial defects
- A number of potentially complicating factors were not included:
  - Thread tolerance deviations
  - Surface roughness and residual stresses
  - Corrosion
- A single flange geometry has been considered – additional investigation would be required to assess LTF and SIF behaviour for other geometries